Human RNA Nm-MTase FTSJ1: new tRNA targets and role in the regulation of brain-specific genes.

Dilyana G. Dimitrova[1], Mira Brazane[1], Tao Ye[2], Virginie Marchand[3], Elise Schaefer[2], Zornitza Stark[4], Martin Delatycki[5], Tracy Dudding[6], Jozef Gecz[7], Laure Teysset[1], Amélie Piton[2], Yuri Motorin[8] and Clément Carré[1,#].

[1]Transgenerational Epigenetics & small RNA Biology, Sorbonne Université, Centre National de la Recherche Scientifique, Laboratoire de Biologie du Développement - Institut de Biologie Paris Seine, 9 Quai Saint Bernard, 75005 Paris, France.
[2]Institute of Genetics and Molecular and Cellular Biology, Strasbourg University, CNRS UMR7104, INSERM U1258, 67400 Illkirch, France.
[3]Université de Lorraine, CNRS, INSERM, EpiRNASeq Core Facility, UMS2008/US40 IBSLor ,F-54000 Nancy, France.
[4]Australian Health and Medical Research Institute, Adelaide, South Australia, 5000, Australia. Victorian Clinical Genetics Services, Murdoch Children's Research Institute, Melbourne, VIC, Australia. The University of Melbourne, Melbourne, VIC, Australia.
[5]Bruce Lefroy Centre for Genetic Health Research, Murdoch Children's Research Institute, Parkville, 3052, Australia.Physiotherapy Department, Monash Health, Cheltenham, Australia. Department of Paediatrics, The University of Melbourne, Parkville, Australia. School of Psychological Sciences, Monash University, Clayton, Australia. Victorian Clinical Genetics Services, Melbourne, Australia.
[6]Genetics of Learning Disability, Hunter Genetics, Waratah, NSW 2298, Australia.
[7]Adelaide Medical School and Robinson Research Institute, The University of Adelaide; South Australian Health and Medical Research Institute, Adelaide, South Australia, 5000, Australia.
[8]Université de Lorraine, CNRS, UMR7365 IMoPA, F-54000 Nancy, France.
[#]Correspondence: clement.carre@gmail.com; clement.carre@sorbonne-universite.fr

ABSTRACT

FTSJ1 is a phyllogenetically conserved human 2'-O-methyltransferase (Nm-MTase) which modifies position 32 as well as the wobble position 34 in the AntiCodon Loop (ACL) of specific tRNAs: $tRNA^{Phe(GAA)}$, $tRNA^{Trp(CCA)}$ and $tRNA^{Leu(UAA)}$. FTSJ1's loss of function has been linked to Non-Syndromic X-Linked Intellectual Disability (NSXLID), and more recently in cancers. However, the exact molecular mechanisms underlying FTSJ1-related pathogenesis are unknown and a potential extended variety of FTSJ1's tRNA targets hasn't been fully addressed yet. We performed unbiased and comprehensive RiboMethSeq analysis of the Nm profiles for human tRNA population extracted from cells derived from NSXLID patients' blood bearing various characterized loss of function mutations in FTSJ1. In addition, we reported a novel FTSJ1 pathogenic variant from a NSXLID patient bearing a *de novo* mutation in the *FTSJ1* gene. Some of the newly identified FTSJ1's tRNA targets are also conserved in *Drosophila* as shown by our previous study on the fly homologues Trm7_32 and Trm7_34, whose loss affects small RNA silencing pathways. In the current study, we reveal a conserved deregulation in both the miRNA and mRNA populations when FTSJ1 function is compromised. In addition, a cross-analysing between deregulated miRNA and mRNA obtained in FTSJ1 mutants highlighted upregulation of *miR10a-5p* which has the capacity to silence the *SPARC* gene mRNA, downregulated in FTSJ1 mutant cells. This suggests that FTSJ1 loss may influence gene expression deregulation by modulation of miRNA silencing. A gene-ontology (GO) enrichment analysis of the deregulated mRNAs primarily matched to brain morphogenesis terms, followed by metabolism and translation related genes. In parallel, the deregulated miRNAs are mostly known for their implication in brain functions and cancers. Based on these results, we suggest that miRNA silencing variations may play a role in the pathological mechanisms of FTSJ1-dependent NSXLID. Finally, our results highlight *miR-181a-5p* as a potential companion diagnostic test in clinical settings for FTSJ1-related intellectual disability.

INTRODUCTION

RNA modifications represent a post-transcriptional layer of gene expression regulation and are the focus of studies of the emerging field of epitranscriptomics (Saletore et al. 2012; Angelova et al. 2018; Zhao et al. 2020). Thanks to their variety and dynamic nature, RNA modifications provide the advantage to rapidly adapt gene expression in response to programmed developmental changes or to unpredictable environmental variations. One of the most abundant RNA modifications is 2'-O-methylation (ribose methylation, Nm) which can affect properties of RNA molecules in multiple ways (*e.g.*, stability, interaction, function) (Kawai et al. 1992; Kurth and Mochizuki 2009; Lacoux et al. 2012). Nm residues are abundant in ribosomal RNAs (rRNAs) and transfer RNAs (tRNAs) (Erales et al. 2017; Marchand et al. 2017), but are also found in other RNA types such as small nuclear RNA (snRNA) (Darzacq 2002; Dai et al. 2017), small non-coding RNA (sncRNA) (Junjie Li et al. 2005; Yu et al. 2005; Horwich et al. 2007; Saito et al. 2007; Kurth and Mochizuki 2009) and messenger RNA (mRNA) (Darzacq 2002; Dai et al. 2017; Bartoli et al. 2018 n.d.). Many Nm positions are conserved through evolution and their presence is essential for maintaining healthy physiological functions. The loss of certain Nm modifications and/or Nm-modifying enzymes has been associated with various pathological conditions (reviewed in (Dimitrova, Teysset, and Carré 2019)), among which cancers (Liu et al. 2017; El Hassouni et al. 2019; Q. He et al. 2020; Marcel et al. 2020) and brain diseases (Jia, Mu, and Ackerman 2012; Abe et al. 2014; Guy et al. 2015; Cavaillé 2017) stand out the most.

FTSJ1 is a human tRNA 2'-O-methyltransferase (Nm-MTase) and a part of the large phylogenetically conserved superfamily of Rrmj/fibrillarin RNA methyltransferases (Bügl et al. 2000; Feder et al. 2003). FTSJ1 homolog in *Saccharomyces cerevisiae* is called Trm7 (tRNA methyltransferase 7), and expression of human FTSJ1 suppresses the severe growth defect of yeast Δ*trm7* mutants (Guy and Phizicky 2015). A substantial part of the original knowledge on FTSJ1's molecular functions has been acquired by the studies done in yeast. In *S. cerevisiae*, Yeast Trm7 2'-O-methylates positions 32 and 34 in the AntiCodon Loop (ACL) of specific tRNA targets: $tRNA^{Phe(GAA)}$, $tRNA^{Trp(CCA)}$ and $tRNA^{Leu(UAA)}$ (Pintard et al. 2002; Guy et al. 2012). To achieve 2'-O-methylation, TRM7 partners with two other proteins: Trm732 for the methylation of a cytosine at position 32, and with Trm734 for the methylation of cytosine or guanine at position 34 (Guy et al. 2012; Jing Li et al. 2020). The presence of both, Cm_{32} and Gm_{34} in $tRNA^{Phe(GAA)}$, is required for efficient conversion of m^1G_{37} to wybutosine (yW_{37}) by other proteins. This molecular circuitry is also conserved in the phylogenetically distinct *Schizosaccharomyces pombe* and in humans (Noma et al. 2006; Guy and Phizicky 2015; Guy et al. 2015; Jing Li et al. 2020).

Recently, our team used the robust and unbiased RiboMethSeq technique to identify two novel non-redundant *Drosophila melanogaster* homologs of human FTSJ1 and yeast Trm7. Flies Trm7_32 and Trm7_34 modify respectively positions 32 and 34 in the ACL on $tRNA^{Phe(GAA)}$, $tRNA^{Trp(CCA)}$ and $tRNA^{Leu(CAA)}$ (Angelova and Dimitrova et al. 2020). Testing the totality of *Drosophila* tRNAs using RiboMethSeq also led to the discovery of novel tRNA targets for these TRM7 family enzymes ($tRNA^{Gln(CUG)}$ and $tRNA^{Glu(CUC)}$), and raised the question about their conservation in humans. Shortly after our publication, it was reported that, similarly to flies, human FTSJ1 modifies position 32 of another $tRNA^{Gln}$ isoacceptor, $tRNA^{Gln(UUG)}$ (Jing Li et al. 2020). This study performed in HEK293T cells tested a selected subset of tRNAs using tRNA purification followed by MS analysis. It was shown that position 32 of $tRNA^{Arg(UCG)}$, $tRNA^{Arg(CCG)}$ and $tRNA^{Arg(ACG)}$ as well as position 34 on $tRNA^{Arg(CCG)}$ and $tRNA^{Leu(CAG)}$ are also 2'-O-methylated by human FTSJ1. $tRNA^{Arg(ACG)}$ was originally identified as a target of fly Trm7_32 (Angelova and Dimitrova et al. 2020), while human $tRNA^{Leu(CAA)}$ (Kawarada et al. 2017) and yeast $tRNA^{Leu(UAA)}$ (Guy et al. 2012) were predicted targets of FTSJ1 and Trm7 respectively.

However, comprehensive and unbiased analysis of all possible FTSJ1 tRNA targets was not yet performed, particularly in human patients samples. This leaves the full spectrum of FTSJ1 tRNA substrates yet to be identified. With the growing knowledge on the biological importance of Nm and the already well-established link between FTSJ1's loss of function and NSXLID (Freude et al. 2004; Ramser et al. 2004; Froyen et al. 2007; Guy et al. 2015), it is becoming urgent to reveal any "hidden" tRNA targets of this enzyme in human.

Males patients bearing an hemizygous loss of function variant in the *FTSJ1* gene suffer from significant limitations both in intellectual functioning and in adaptive behavior. Similar phenotypes including impaired learning and memory capacity were recently observed in *FTSJ1* KO mice that also present a reduced body weight and bone mass, as well as altered energy metabolism (Jensen et al. 2019). In flies, we recently showed that the loss of Trm7_32 and Trm7_34 provokes reduced lifespan and body weight, and RNAi antiviral defenses, associated with a locomotion defect which may be explained, at least partially, by impaired sncRNA silencing pathways (Angelova and Dimitrova et al. 2020). Finally, yeast Δ*trm7* mutants grow poorly due to a constitutive general amino acid control (GAAC) activation as well as to the possible reduced availability of aminoacylated $tRNA^{Phe}$ (Pintard et al. 2002; Guy et al. 2012; Han et al. 2018). In mammals, however, the evidence relating FTSJ1 to translation is yet scarce and one linking it to sncRNA silencing is missing. The molecular and cellular mechanisms underlying NSXLID pathogenesis are not yet fully understood.

In this study, we first aimed to identify the panel of FTSJ1's tRNA targets in human lymphoblastoid cell lines (LCLs) directly derived from blood samples of NSXLID male patients bearing loss of function variants in *FTSJ1* gene *vs.* male individuals with intact FTSJ1 activity. The Nm profiles of the totality of human tRNAs was evaluated by the unbiased RiboMethSeq method (Marchand et al. 2016a, 2017) in FTSJ1 loss of function *vs.* functional FTSJ1 context. Importantly, most of the previously reported substrates ($tRNA^{Phe(GAA)}$, $tRNA^{Trp(CCA)}$, $tRNA^{Leu(CAG)}$ and $tRNA^{Arg(UCG)}$) were confirmed with nucleotide position precision. Previously, the enzymatic activity of FTSJ1 on selected tRNAs has been revealed through HPLC (High-Performance Liquid Chromatography) (Guy et al. 2015) and more recently through UPLC-MS/MS (Ultra-Performance Liquid Chromatography–Mass Spectrometry/Mass Spectrometry) (Jing Li et al. 2020). Both approaches analyse individual nucleosides of selected tRNAs based on already reported sequences. The exact position of the modified nucleotide is thus inferred from available information on tRNA sequences and modification profiles (Chan and Lowe 2016; Boccaletto et al. 2018). Therefore, the contribution of the current report consists in the precise mapping of FTSJ1-dependent Nm, while considering the totality of expressed human tRNA isotypes and isoacceptors without any selection biases or possible missing information on presently available databases. An additional advantage of the RiboMethSeq is that it enables to "scan" every nucleotide position in all expressed tRNAs in one single experiment. Thus, unchanged Nm on tRNAs between the tested conditions can be used as internal control, and demonstrates here the high specificity of FTSJ1 for positions 32 and 34 in the ACL of tRNA targets.

Our previous study in *Drosophila melanogaster* revealed tRNA substrates for Trm7_32 (C_{32} in $tRNA^{Arg(ACG)}$, $tRNA^{Gln(CUG)}$, $tRNA^{Glu(CUC)}$ and $tRNA^{Va(AAC)}$) for which, at the time of publication, there was no experimental evidence identifying them as targets of human FTSJ1 nor yeast Trm7 (Angelova and Dimitrova et al. 2020). This, together with the additional freshly identified targets of human FTSJ1 by (Jing Li et al. 2020), raised the suspicion for an expanded tRNA targets panel for these enzymes compared to what was previously known. Here we give reason to this suspicion by showing the conservation of C_{32} in $tRNA^{Gln(CUG)}$ as substrate of human FTSJ1, and also revealing an additional target: U_{32} in $tRNA^{Gly(CCC)}$, while confirming previously and recently reported ones.

In addition, through illumina sequencing transcriptome analysis we report deregulations of mRNA and miRNA populations in FTSJ1-lacking NSXLID patients' LCLs. A cross analysis of mRNA and miRNA datasets and experimental databases for identification of miRNA targets revealed potential miRNA::mRNA target interactions in the NSXLID patients' LCLs. Considering the sncRNA silencing impairment in FTSJ1 ortologs deficient

flies (Angelova and Dimitrova et al. 2020), these results suggest a conserved molecular phenotype in humans lacking FTSJ1.

Importantly, most of the differentially expressed mRNAs between healthy individuals and patients with *FTSJ1* variants are implicated in brain morphogenesis as revealed by Gene Ontology (GO) analysis, and most of the differentially expressed miRNAs are implicated in brain-related functions and cancers, including glioblastoma.

Collectively, our study suggests perturbation of sncRNA silencing mechanisms implicated in FTSJ1-related NSXLID pathogenesis through the link with FTSJ1's Nm-MTase activity. Finally, we propose *miRNA-181a-5p* as a potential future biomarker of FTSJ1 NSXLID that seems to be specifically and significantly over-represented in FTSJ1 patients' cells.

MATERIALS & METHODS

FTSJ1 variants and lymphoblastoid cell lines (LCL)

The various lymphoblastoid cell lines (LCLs) were generated by using classical methods from blood samples of NSXLID male patients or healthy male individuals. The cells were cultured in RPMI-1640 medium with L-glutamine and sodium bicarbonate (ref. R8758-500ML, SIGMA) supplemented with 10% FBS (Gibco) and 1% penicillin–streptomycin (ref. P0781, SIGMA) at 37 °C with 5% CO_2. Cells were split at ½ dilution approximately 24h before being collected for RNA extraction with TRI-Reagent (Sigma Aldrich) following the manufacturer's instructions.

6514AW & 6514JW (LCL65AW & LCL65JW in this study): Family A3 - LCLs from two brothers with mild or severe ID associated with psychiatric manifestations (anger, aggression, anxiety, depression, schizophrenia requiring medication) bearing a splice variant in *FTSJ1:* c.121+1delG (Freude et al. 2004). This variant leads to a retention of intron 2 creating a premature stop codon (p.Gly41Valfs*10). Part of the transcripts undergo nonsense mRNA decay.

11716IJ (LCL11 in this study): Family A18 - LCL for one male with moderate to severe mental retardation without dysmorphic features carrying an interstitial microdeletion at Xp11.23. The extent of the deletion was subsequently delineated to about 50 kb by regular PCR and included only the *SLC38A5* and *FTSJ1* genes. qPCR with the FTSJ1-ex3 primers is negative, thus demonstrating the complete deletion of FTSJ1 locus (Froyen et al. 2007).

22341SR (LCL22 in this study): Family 7 (A26P) - LCL for one male with moderate ID and psychiatric features (mild anxiety and compulsive behavior) carrying a missense mutation c.76G>C; p.Ala26Pro in *FTSJ1*. This family has been reported previously (Guy et al. 2015) .

LCL-MM: This is a newly reported family. The LCL has been generated from one male with mild ID and behavioral problems carrying a hemizygous variant c.362-2A>T; p.? in *FTSJ1*. The mutation is predicted to disrupt the acceptor splice site of exon 6. This variant might cause a skipping of the entire exon in the mRNA leading to a frameshift. It shows a strong decrease of the corresponding mRNA. This variant was deposited in ClinVar database (VCV000981372.1).

18451PK (LCL18 in this study), 16806JD (LCL16 in this study), 3-2591 (LCL25 in this study) and 3-5456 (LCL54 in this study): LCL established from control males. 4 LCL's not mutated in the *FTSJ1* gene from unaffected males of similar age were used as control.

RiboMethSeq

RiboMethSeq analysis of human LCL tRNAs was performed as described in (Marchand et al. 2017). Briefly, tRNAs extracted from LCLs were fragmented in 50 mM bicarbonate buffer pH 9.2 for 15 minutes at 95°C. The reaction was stopped by ethanol precipitation. The pellet was washed with 80% ethanol and sizes of generated RNA fragments were assessed by capillary electrophoresis using a small RNA chip on Bioanalyzer 2100 (Agilent, USA). RNA fragments were directly 3'-end dephosphorylated using 5 U of Antarctic Phosphatase (New England Biolabs, UK) for 30 minutes at 37°C. After inactivation of the phosphatase for 5 minutes at 70°C, RNA fragments were phosphorylated at the 5'-end using T4 PNK and 1 mM ATP for one hour at 37°C. End-repaired RNA fragments were then purified using RNeasy MinElute Cleanup kit (QIAGEN, Germany) according to the manufacturer's recommendations. RNA fragments were converted to library using NEBNext® Small RNA Library kit (ref#E7330S, New England Biolabs, UK or equivalent from Illumina, USA) following the manufacturer's instructions. DNA library quality was assessed using a High Sensitivity DNA chip on a Bioanalyzer 2100. Library sequencing was performed on Illumina HiSeq 1000 in single-read mode for 50 nt. Primary analysis of sequencing quality was performed with RTA 2.12 software, to insure > Q30 quality score for > 95 % of obtained sequences.

Following SR50 sequencing run, demultiplexing was performed with BclToFastq v2.4, reads not passing quality filter were removed. Raw reads after demultiplexing were trimmed with Trimmomatic v0.32 (Bolger, Lohse, and Usadel 2014). Alignment to the reference tDNA sequences was performed with bowtie 2 ver2.2.4 (Langmead et al. 2009) in End-to-End mode. Uniquely mapped reads were extracted from *sam file by RNA ID and converted to *.bed format using bedtools v2.25.0 (Quinlan 2014). Positional counting of 5'-and 3'-ends of each read was performed with awk Unix command. Further treatment steps were performed in R environment (v3.0.1). In brief, 5'-and 3'-end counts were merged together by RNA position and used for calculation of ScoreMEAN (derived from MAX Score (Pichot et al. 2020), as well as Scores A and B (Birkedal et al. 2015) and MethScore (Marchand et al. 2016b). Scores were calculated for two neighboring nucleotides. Profiles of RNA cleavage at selected (candidate and previously known) positions were extracted and visually inspected.

mRNA sequencing

mRNA sequencing was performed as in (Khalil et al. 2018). 5 µg of total RNA were treated by 1MBU of DNAse (BaseLine-Zero™ DNAse, Epicentre, USA) for 20 min at 37 °C

to remove residual genomic DNA contamination. RNA quality was verified by PicoRNA chip on Bioanalyzer 2100 (Agilent, USA) to ensure RIN (RNA Integrity Number) > 8.0. PolyA + fraction was isolated from 4.5 µg of DNAse-treated total RNA using NEBNext Oligo d(T)25 Magnetic beads kit (NEB, USA), according to manufacturer's recommendations. PolyA + enrichment and the absence of residual rRNA contamination were verified using PicoRNA chips on Bioanalyzer 2100 (Agilent, USA). PolyA + fraction (1 ng for each sample) was used for whole-transcriptome library preparation using ScriptSeq v2 RNA-Seq kit (Illumina, USA). Libraries amplified in 14 PCR cycles were purified using Agencourt AMPure XP beads (Beckman-Coulter, USA), at a ratio 0.9x to remove adapter dimer contamination. Quality of the libraries was verified by HS DNA Chip on Bioanalyzer 2100 (Agilent, USA) and quantification done by Qubit 2.0 with appropriate RNA quantification kit. Sequencing was performed on HiSeq1000 (Illumina, USA) in single read SR50 mode. About 50 million of raw sequencing reads were obtained for each sample. Adapters were trimmed by Trimmomatic v0.32 (Bolger, Lohse, and Usadel 2014) and the resulting sequencing reads aligned in sensitive-local mode by Bowtie 2 v2.2.4 (Langmead and Salzberg 2012) to hg19 build of human genome. Differential expression was analyzed using *.bam files in DESeq2 package (Love, Huber, and Anders 2014) under R environment. Analysis of KEGG and Gene Ontology pathways for differentially expressed genes was done under R environment.

small RNA sequencing and data analysis

Small RNA-Seq libraries were generated from 1000 ng of total RNA using TruSeq Small RNA Library Prep Kit (Illumina, San Diego, CA), according to manufacturer's instructions. Briefly, in the first step, RNA adapters were sequentially ligated to each end of the RNA, first the 3' RNA adapter that is specifically modified to target microRNAs and other small RNAs, then the 5' RNA adapter. Small RNA ligated with 3' and 5' adapters were reverse transcribed and PCR amplified (30 sec at 98ºC; [10 sec at 98ºC, 30 sec at 60ºC, 15 sec at 72ºC] x 13 cycles; 10 min at 72ºC) to create cDNA constructs. Amplified cDNA constructs of 20 to 40 nt were selectively isolated by acrylamide gel purification followed by ethanol precipitation. The final cDNA libraries were checked for quality and quantified using capillary electrophoresis and sequenced on the Illumina HiSeq 4000 at the Institut de Génétique et de Biologie Moléculaire et Cellulaire (IGBMC) GenomEast sequencing platform.

For small RNA data analysis, adapters were trimmed from total reads using FASTX_Toolkit [http://hannonlab.cshl.edu/fastx_toolkit/]. Only trimmed reads with a length between 15 and 40 nucleotides were kept for the further analysis.

Data analysis was performed according to published pipeline ncPRO-seq [https://www.ncbi.nlm.nih.gov/pubmed/23044543]. Briefly, reads were mapped onto the human genome assembly hg19 with Bowtie v1.0.0. The annotations for miRNAs were done with miRBase v21. The normalization and comparisons of interest were performed using the test for differential expression, proposed by (Love, Huber, and Anders 2014) and implemented in the Bioconductor package DESeq2 v1.22.2 [http://bioconductor.org/]. MicroRNA target prediction was performed using miRNet 2.0 [https://www.mirnet.ca/miRNet/home.xhtml]

Northern blotting

For northern blotting analysis of tRNA, 5 µg of total RNA from human LCLs were resolved on 15 % urea-polyacrylamide gels for approximately 2h in 0.5x TBE buffer at 150 V, then transferred to Hybond-NX membrane (GE Healthcare) in 0,5x TBE buffer for 1h at 350 mA of current and EDC-cross-linked for 45 min at 60°C with a solution containing 33 mg/ml of 1-ethyl-3-(3-dimethylaminopropyl)carbodiimide (EDC) (Sigma Aldrich), 11 ng/ul of 1-methylimidazol and 0.46% of HCl. The membranes were first pre-hybridized for 1h at 42°C in a hybridization buffer containing 5xSSC, 7% SDS, 5.6 mM NaH_2PO_4, 14.4 mM Na_2HPO_4 and 1x Denhardt's solution. DNA oligonucleotide probes were labelled with ^{32}P at the 5'-end by T4 polynucleotide kinase following manufacturer's instructions (Fermentas). The membranes were hybridized with the labelled probes overnight at 42°C in the hybridization buffer, then washed twice for 15 min in wash buffer A (3x SSC and 5% SDS) and twice in wash buffer B (1x SSC and 1% SDS) before film exposure at -80°C for variable time durations. Probe sequences are available in the *Primers and Probes section*.

RT-qPCR

RNA was extracted from human LCLs using TRI-Reagent (Sigma Aldrich). After DNase digestion of total RNA using the TURBO DNA-free™ Kit (Ambion), 1 µg was used in a reverse transcription reaction with Random Primers (Promega) and RevertAid Reverse Transcriptase (ref. EP0442, Thermofisher). The cDNA was used to perform qPCR on a CFX96 Touch™ Real-Time PCR Detection System (Bio Rad) using target-specific primers. *hGAPDH* was used for normalization (*Primers and Probes section*). The analysis was performed using ΔΔ Ct, on three biological replicates. Statistical analysis using a bilateral Student's t-test was performed and *p*-values were calculated.

Primers and Probes

Northern blot analysis was performed with the use of hsa-miR-181a-5p specific probes with the following sequences: 5'-AACATTCAACGCTGTCGGTGAGT-3' (sense probe) and 5'-ACTCACCGACAGCGTTGAATGTT-3' (antisense probe). Human U6 specific probe was used for detecting U6 as a loading control: 5'-GCAAGGATGACACGCAAATTCGTGA-3' (sense probe) and 5'-TCACGAATTTGCGTGTCATCCTTGC-3' (antisense probe).

qPCR analysis (after an RT reaction performed with random primers) were performed with the use of primers with the following sequences:

Target Gene	Primer's sense	Sequence
BTBD3	Forward	5'-TGGCAGATGTACATTTTGTGG-3'
	Reverse	5'-AACACAGAGCTCCCAACAGC-3'
SPARC	Forward	5'-GAGAAGGTGTGCAGCAATGA-3'
	Reverse	5'-AAGTGGCAGGAAGAGTCGAA-3'
GAPDH	Forward	5'-CAACGGATTTGGTCGTATTGG-3'
	Reverse	5'-GCAACAATATCCACTTTACCAGAGTTAA-3'
FTSJ1	Forward	5'-CCATTCTTACGACCCAGATTTCA-3'
	Reverse	5'-CCCTCTAGGTCCAGTGGGTAAC-3'

RESULTS

New tRNA targets of human FTSJ1

To identify new potential tRNA targets of human FTSJ1, we compared the Nm modification profiles of positions 32 and 34 for all detectable tRNA species using the RiboMethSeq (Marchand et al. 2017) on human LCLs obtained from control individuals (n=4) *vs.* LCLs obtained from individuals with ID harboring loss-of-function variants in *FTSJ1* (n=5, from four unrelated families) (Figure. 1a). Four of these patients were already reported and harbor: a splice variant leading to a premature stop codon (Freude et al. 2004) (LCL65AW and LCL65JW), a deletion encompassing *FTSJ1* together with another gene (Froyen et al. 2007) (LCL11), and a missense variant (p.Ala26Pro) affecting an amino acid located close to FTSJ1 catalytic pocket resulting in loss of Gm_{34}, but not of Cm_{32} in human $tRNA^{Phe}$ (Guy et al. 2015) (LCL22), similarly to what is observed in a *Drosophila* Trm7_34 single mutant (Angelova and Dimitrova et al. 2020). The last individual was not reported nor characterized before: he presents mild ID and behavioral manifestations and harbors a *de novo* pathogenic variant affecting the consensus acceptor splice site of exon 6 (NM_012280.3: c.362-2A>T) (LCL-MM). This mutation is predicted to lead to the skipping of exon 6 inducing a frameshift, most probably resulting in a premature stop codon thus promoting cleavage of the mRNA through Nonsense Mediated mRNA Decay (NMD). Accordingly, *FTSJ1* mRNA steady state level in LCL-MM is significantly reduced when compared to LCL from control individuals (Figure. S1a).

tRNAPhe(GAA)			
Individual	**Cm32**	**Gm34**	**LCL code name**
Control individuals	Yes	Yes	LCL16
			LCL18
			LCL24
			LCL54
Affected individuals with FTSJ1 variant	Yes	No	LCL22
	No		LCL65AW
			LCL65JW
			LCL11
			LCLMM

Figure 1a. FTSJ1 targets tRNA-Phe at positions 32 and 34 in humans. Control and affected FTSJ1 individuals Nm status at positions 32 and 34 of human $tRNA^{Phe}$.

To obtain a comprehensive picture of the Nm-MTase specificity for FTSJ1 *in vivo*, we performed tRNA RiboMethSeq analysis on LCLs isolated from patients carrying a pathogenic variant in *FTSJ1* and control individuals. RiboMethSeq allows tRNA-wide Nm detection based on random RNA fragmentation by alkaline hydrolysis followed by library preparation and sequencing (Marchand et al. 2017). The presence or absence of Nm can be appreciated from characteristic coverage profiles of the 5′-/3′-ends of obtained cDNAs. Since Nm residues protect the adjacent 3′-phosphodiester bond to the neighbouring nucleotide from hydrolysis, a gap in the coverage at the n+1 position indicates the presence of a 2′-O-methylated nucleotide at position n. As an example, when analyzing the 2′-O-methylation status at position 34 for $tRNA^{Phe}$ in control individuals, reads at position 35 (equals n+1) were under-represented in regard to their direct nucleotide neighbors. Depicted MethScores (Figure. 1b) were calculated for two neighboring nucleotides (Marchand et al. 2016a).

These results confirmed the known FTSJ1 targets ($tRNA^{Phe(GAA)}$ and $tRNA^{Trp(CCA)}$) and located the FTSJ1-deposited Nm modifications to their predicted positions in the ACL (C_{32} and N_{34}, Figure. 1b). However, Cm_{32} of $tRNA^{Phe(GAA)}$ made an exception and no detectable Nm MethScore variations between control and mutant FTSJ1 cells were found using RiboMethSeq MethScore analysis. The analysis of this position was challenging due to low read numbers necessary for its quantification. Therefore, we do not exclude that the parallel loss of Gm_{34} in *FTSJ1* mutated cells is provoking the unchanged MethScore at position 32. However, when looking at raw reads count profil, reads at position 33 (Cm_{32}) are increasing in *FTSJ1* mutated cells (Figure. S1b) denoting a loss of Nm deposition in FTSJ1 mutated LCLs. Importantly, we previously reported that $tRNA^{Phe(GAA)}$ ACL positions are challenging to detect with Ribomethseq, mostly due to the hyper-modification on position 37 of $tRNA^{Phe}$ (Angelova and Dimitrova et al. 2020). Indeed, $o2yW_{37}$/ m^1G_{37} impairs reverse transcription thereby reducing the number of cDNAs spanning the ACL.

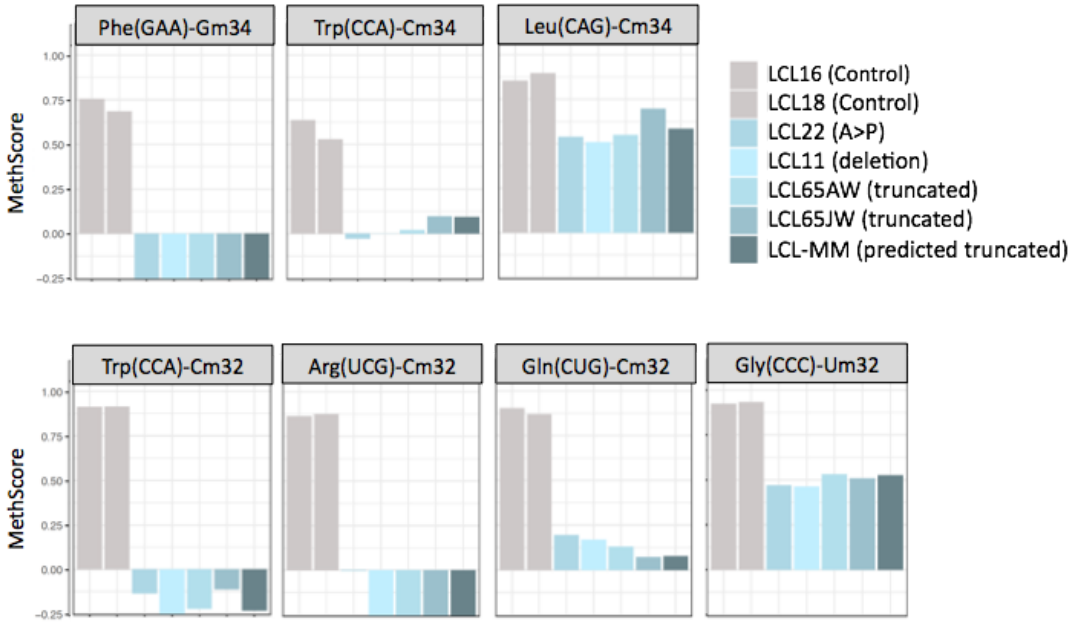

Figure 1b. FTSJ1 targets multiple tRNAs at positions 32 and 34 in humans. Methylation scores (MethScore) for 2'-O-methylated positions in tRNAs showing altered methylation in FTSJ1 loss-of-function mutant LCLs. MethScore (Score C), representing the level of ribose methylation was calculated from protection profiles. Data are shown for positions 32 and 34 in different *H. sapiens* tRNAs as measured in different LCL lines that are indicated with different colour code. Grey: control LCL; blue: *FTSJ1* mutant LCLs.

The RiboMethSeq analysis did not detect variations in Cm_{32} on $tRNA^{Leu(UAA)}$, a tentative FTSJ1 target based on yeast rescue assays using exogenous expression of human FTSJ1 protein in *S. cerevisiae trm7Δ* strain (Guy and Phizicky 2015) as well as on RiboMethSeq data for *Drosophila* orthologue Trm7_32 (Angelova and Dimitrova et al. 2020). However, we found a partial loss of Cm_{34} in a specific subtype of $tRNA^{Leu(CAG)}$ in human LCLs lacking FTSJ1 function. This particular target was only very recently reported in humans by using HEK293T *FTSJ1* KO cells (Jing Li et al. 2020). We also found that FTSJ1 loss of function in human LCLs leads to almost complete loss of Cm_{32} on $tRNA^{Gln(CUG)}$ (Figure. 1b), a recently discovered target of *Drosophila* Trm7_32 (Angelova and Dimitrova et al. 2020) which was not reported on the RNA modification database Modomics for either yeast or humans (Boccaletto et al. 2018). In addition, we detected a notable decrease of Um_{32} in $tRNA^{Gly(CCC)}$ (Figure. 1b), a modification previously reported on Modomics, however the enzyme responsible for it was up to now unknown. Cm_{32} on human $tRNA^{Arg(UCG)}$ has been reported only recently (Jing Li et al. 2020). Our RiboMethSeq analysis shows that Cm_{32} on $tRNA^{Arg(UCG)}$ was abolished in all LCLs lacking proper FTSJ1 function, while Um_{32} on $tRNA^{Gly(CCC)}$ was partially but significantly affected (~ 50%, Figure. 1b) and was not described yet in previous reports.

Those experiments performed without any selection on whole tRNAs expressed in LCL derived from NSXLID patients' blood cells confirmed most of the already known tRNAs target positions of human FTSJ1 and uncovered novel, not yet reported human FTSJ1 tRNA targets (Figure. 1c).

tRNA target	*Humans*				*Drosophila*		*S. cerevisiae*	
	Current RiboMethSeq study		Previous MS studies		RiboMethSeq study		MS studies	
	Position 32	*Position 34*	*Position 32*	*Position 34*	*Position 32*	*Position 34*	*Position 32*	*Position 34*
Arg(UCG)	Cm	no	Cm	no	no	no	n.d.	n.d.
Arg(ACG)	no	no	Cm	no	Cm	no	n.d.	n.d.
Arg(CCG)	no	no	Um	Cm	no	no	n.d.	n.d.
Leu(CAG)	no	Cm	n.d.	Cm	no	no	n.d.	n.d.
Leu(CAA)	no	no	n.d.	Cm	Cm	Cm	n.d.	n.d.
Leu(UAA)	no	no	n.d.	no	no	no	Cm	Cm
Leu(AAG)	no	no	n.d.	no	no	no	n.d.	n.d.
Leu(UAG)	no	no	n.d.	no	no	no	n.d.	n.d.
Phe(GAA)	no	Gm	Cm	Gm	no	Gm	Cm	Gm
Trp(CCA)	Cm	Cm	Cm	Cm	Cm	Cm	Cm	Cm
Gln(CUG)	Cm	no	n.d.	n.d.	Cm	no	n.d.	n.d.
Gln(UUG)	no	no	Cm	n.d.	no	no	n.d.	n.d.
Gly(CCC)	Um	no	n.d.	no	no	no	n.d.	n.d.
Glu(CUC)	no	no	n.d.	n.d.	Cm	no	n.d.	n.d.
Val(AAC)	no	no	n.d.	n.d.	Cm	no	n.d.	n.d.
Asn((GUU)	no	no	n.d.	n.d.	Cm	no	n.d.	n.d.
Ala(AGC)	no	no	n.d.	n.d.	Um	no	n.d.	n.d.

Figure 1c. FTSJ1 targets multiple human tRNAs at positions 32 and 34. A summary of tRNA nucleotides revealed to date, including by the current study, as targets of human FTSJ1, as well as those targeted by Drosophila Trm7_32 and Trm7_34, and yeast Trm7 in the respective organisms. For the tRNA targets are given the isotype (determined by the bound amino acid) and the isoacceptor (determined by the ACL sequence). In blue are highlighted the studies done with the site-specific RiboMethSeq and in grey, the ones done by mass spectrometry (MS) single nucleotide analysis. n.d. stands for non-determined and indicates that the tRNA was not tested or if tested the data was not analysable. no stands for non-detected Nm. Cm, Gm and Um stand for 2'-O-methylated respectively C, G and U nucleotides.

FTSJ1 loss of function affects the miRNA populations

Our previous work uncovered the *Drosophila* homologs of FTSJ1, Trm7_32 and Trm7_34, and showed that their loss of functions surprisingly leads to perturbations in the small non-coding RNA (sncRNA) gene silencing pathways including the miRNA population (Angelova and Dimitrova et al. 2020). We wanted to investigate whether such perturbations are conserved in NSXLID patient somatic cells lacking proper FTSJ1 function. We thus performed a small RNA sequencing on the 5 LCLs carrying *FTSJ1* loss-of-function variants compared to 4 LCLs from control individuals in order to assess a differential expression analysis of the miRNAs population.

The principal component analysis (PCA) from the different *FTSJ1* loss-of-function cell lines shows a high similarity and thus clusters on the PCA plot, while the wild type lines were more dispersed, possibly explained by their geographic origins and/or age of cell line generation (Figure. S2a). The DESeq2 differential expression analysis showed statistically significant deregulation of 36 miRNAs when comparing FTSJ1 mutants to control LCLs. 17

miRNA were up- and 19 down-regulated (Figures. 2a, S2b and S2c). Importantly, as already reported in *Drosophila*, the results from human LCLs showed that the global miRNA distribution was not drastically affected in FTSJ1 mutant LCLs when compared to controls.

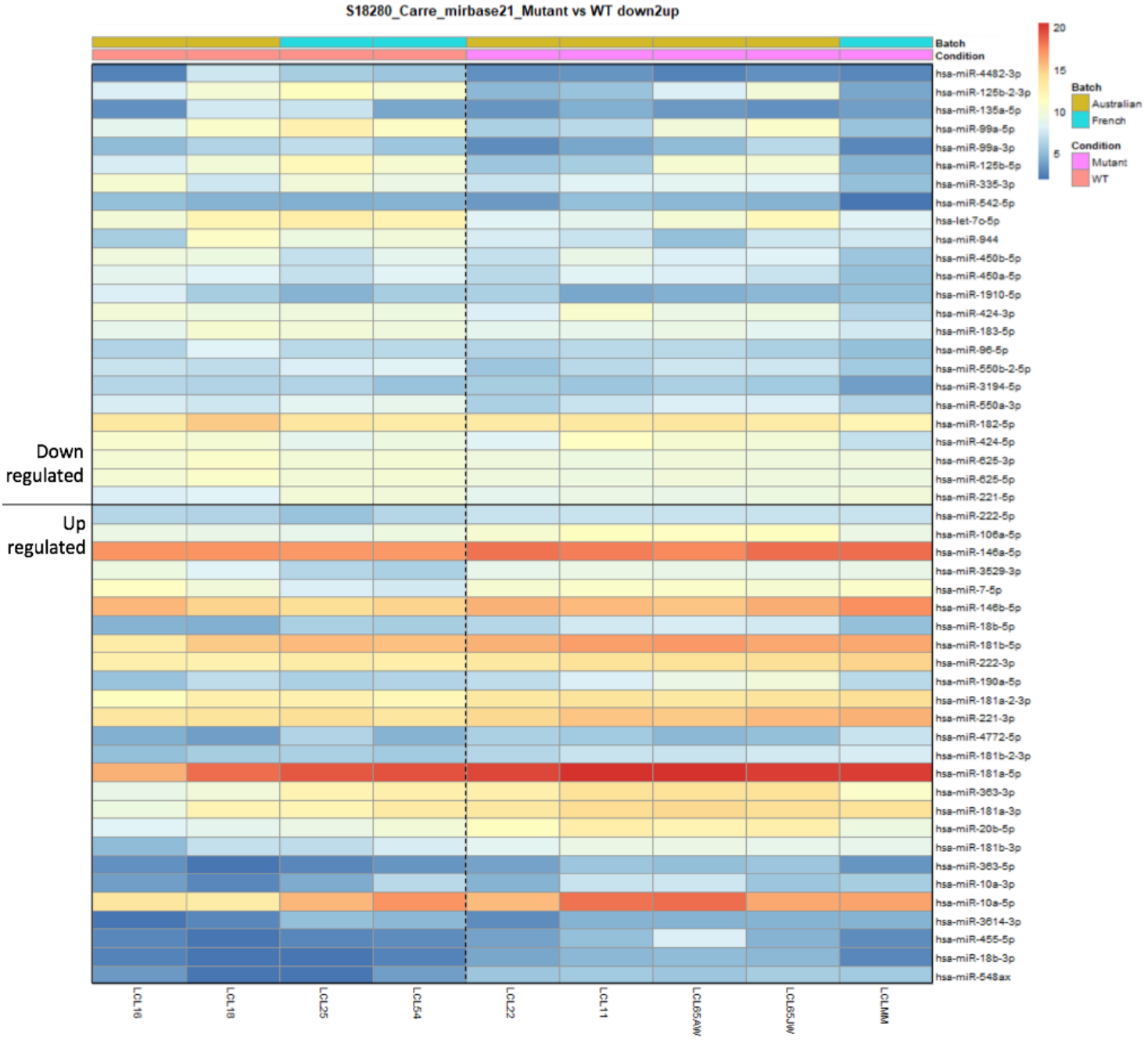

Figure 2a. FTSJ1 loss of function leads to miRNAs deregulation in NSXLID patients LCLs. Heat map generated using the pheatmap package in R showing the 36 deregulated miRNAs in FTSJ1 loss of function LCLs compared to controls. Batch points to the country of origin of the LCLs. Condition points to the FTSJ1 LCL status, WT or mutated for *FTSJ1* gene.

Next, we searched in the literature for evidence of a link between the 36 significantly deregulated miRNAs in FTSJ1 mutated cells and neuronal functions or neurodevelopmental disorders as FTSJ1 patients suffer from intellectual disability due to neurodevelopmental defects. Interestingly, it turned out that 21 of the miRNAs deregulated in the FTSJ1 mutant patient derived cells have been already identified in other small RNAseq studies performed in the context of brain diseases such as epilepsy, Parkinson's and Alzheimer's diseases (Lau et al. 2013; Kretschmann et al. 2015; Ding et al. 2016; Roser et al. 2018). This bibliographic search also revealed that 29 of the deregulated miRNAs in *FTSJ1* mutated LCLs have been linked to different types of cancers (Lund 2010; Watahiki et al. 2011; Y. Li et al. 2015; Khuu et al. 2016; Yang et al. 2017; Jiang et al. 2018), including 21 miRNAs involved specifically in brain-related cancers and mostly in glioblastoma (Gillies and Lorimer 2007; Shi et al. 2008; Lund 2010; Conti et al. 2016) (Figure. 2b and Table. 1).

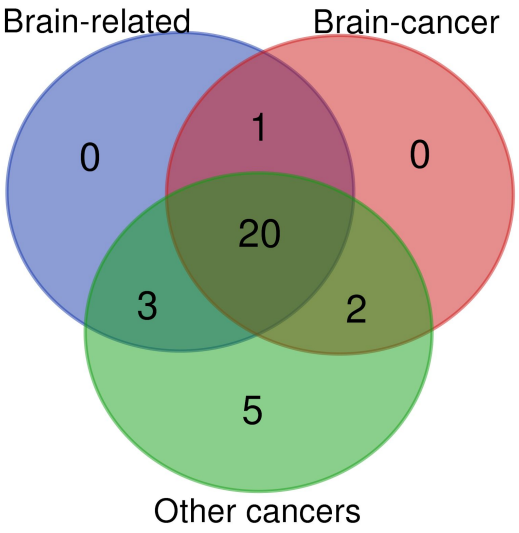

Figure 2b. FTSJ1 loss of function leads to miRNAs deregulation in NSXLID patients LCLs. Bibliographic search (Table. 1) of the miRNAs deregulated in FTSJ1 loss of function LCLs reveals evidence for many of them as being implicated in cancers or brain development and brain diseases. The number of miRNAs related to brain, cancer and brain-cancer specifically are indicated respectively in the blue, green and red circle.
The Venn diagram was generated by http://bioinformatics.psb.ugent.be/webtools/Venn/.

miRNA	Brain-related	Brain-cancer-related	Other cancers
hsa-miR-20b-5p	-	-	doi: 10.2174/2211536605666160322151813
hsa-miR-222-3p	doi: 10.1002/emmm.201201974 doi: 10.1007/s12031-014-0368-6 doi: 10.1007/s00018-012-0992-7 doi: 10.1371/journal.pone.0053464	doi: 10.4161/cc.6.16.4526 doi: 10.1186/1476-4598-9-229	-
hsa-miR-548ax	-	neuroblastoma for other miR-548 familly members	doi: 10.1371/journal.pone.0024950 (also others cancers for other miR-548 familly members)
hsa-miR-125b-2-3p	yes	yes	yes
hsa-miR-221-3p	doi: 10.1007/s12031-014-0368-6 doi: 10.1007/s00018-012-0992-7 doi: 10.1371/journal.pone.0053464 doi:10.1016/j.parkreldis.2015.11.014 doi: 10.1002/cbf.3224 doi:10.3389/fnins.2018.00625	(see miR-222-3p)	doi: 10.1038/onc.2008.178
hsa-miR-335-3p	yes	yes	yes
hsa-miR-181b-2-3p	(see miR(181a-5p)	(see miR(181a-5p)	(see miR(181a-5p)
hsa-miR-99a-5p	yes	yes	yes
hsa-miR-10a-5p	doi:10.18632/oncotarget.6158 doi:10.3389/fnins.2018.00625	doi: 10.4161/rna.8.5.16324 doi: 10.1038/cdd.2009.58	doi: 10.4161/rna.8.5.16324 doi: 10.1038/cdd.2009.58
hsa-miR-181b-3p	(see miR(181a-5p)	(see miR(181a-5p)	(see miR(181a-5p)
hsa-miR-106a-5p	yes	yes	yes
hsa-miR-181a-2-3p	(see miR(181a-5p)	(see miR(181a-5p)	(see miR(181a-5p)
hsa-miR-146a-5p	yes	yes	yes
hsa-miR-4482-3p	-	-	-
hsa-miR-125b-5p	yes	yes	yes
hsa-miR-450b-5p	-	-	yes
hsa-miR-424-3p	yes	-	yes
hsa-miR-363-3p	doi: 10.1002/emmm.201201974 doi: 10.3390/ijms20071665	doi: 10.1007/s13277-016-5273-x doi: 10.1016/j.surg.2013.04.005	doi: 10.3892/mmr.2017.8131 doi: 10.3892/or.2017.6018 doi: 10.1016/j.bbrc.2016.04.055 doi: 10.1111/jcmm.12920 doi: 10.1186/s12885-016-2863-3 doi: 10.1186/s12885-015-1888-3 doi: 10.18632/oncotarget.9169 doi: 10.2174/2211536605666160322151813
hsa-let-7c-5p	-	-	-
hsa-miR-450a-5p	yes	-	yes
hsa-miR-18b-5p	-	-	-
hsa-miR-550a-3p	-	-	yes
hsa-miR-181a-5p	doi: 10.1038/s41598-017-09095-3 doi:10.1016/j.parkreldis.2015.11.014 doi:10.3389/fnins.2018.00625	doi:10.1016/j.brainres.2008.07.085	doi: 10.1159/000485351 doi: 10.1158/0008-5472.CAN-14-2875
hsa-miR-550b-2-5p	-	-	yes
hsa-miR-181a-3p	(see miR(181a-5p)	(see miR(181a-5p)	(see miR(181a-5p)
hsa-miR-181b-5p	(see miR(181a-5p)	(see miR(181a-5p)	(see miR(181a-5p)
hsa-miR-183-5p	yes	yes	yes
hsa-miR-99a-3p	yes	yes	yes
hsa-miR-135a-5p	yes	yes	yes
hsa-miR-146b-5p	yes	yes	yes
hsa-miR-542-5p	-	yes	yes
hsa-miR-944	yes	-	yes
hsa-miR-625-5p	-	-	-
hsa-miR-625-3p	-	-	-
hsa-miR-4772-5p	-	-	yes
hsa-miR-182-5p	yes	yes	yes
Total #	24	23	30

Table 1. Bibliographic search on miRNA deregulated in FTSJ1 loss-of-function LCL mutant cell line. The list shows for each miRNA if any link was found to brain development or brain-related diseases, also cancer and specifically to brain-cancers. The doi is given as reference for most of the miRNAs. The color code of the miRNA names indicates if they were found to be up- (red) or down-regulates (blue) in FTSJ1 mutant LCLs derived from NSXLID patients compared to control LCLs derived from healthy individuals.

Next, we selected a representative and disease-relevant subset of the deregulated miRNAs based on their fold change and level of expression. To verify the small RNAseq relevance, four hemizygous FTSJ1 LCLs (control) and five LCLs mutants for FTSJ1 were analyzed by northern blotting with a specific probe complementary to *miRNA-181a-5p*, a miRNA reported to be involved in vascular inflammation and atherosclerosis (Su et al. 2019), and found expressed in neuronal cells in mammals (Dostie et al. 2003). One clear hybridization signal was observed in all FTSJ1 mutant LCLs corresponding to mature *miRNA-181a-5p* (~25 nt, Figure. 2c). In contrast, the 4 control LCLs show a weak signal on the northern blot membrane even after image over-exposure (Figures. 2c and S2d).

Together with the small non-coding RNA sequencing differential expression analyses (Figure. 2a), this northern blot experiment demonstrates that FTSJ1 function affects some miRNA steady state levels and suggests that the deregulation of miRNA-mediated gene silencing observed in all FTSJ1 mutated LCLs was not caused by a global failure in miRNA biogenesis (Figure. 2a, S2b and S2c).

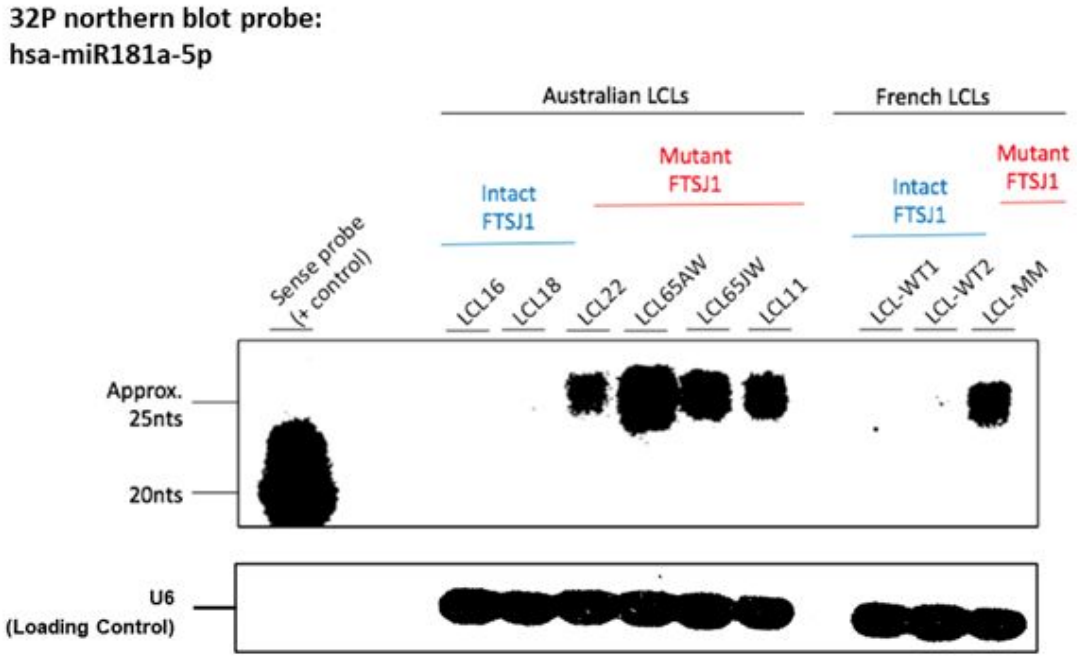

Figure 2c. FTSJ1 loss of function leads to miRNAs deregulation in NSXLID patients LCLs. Northern blot analysis with ^{32}P-labelled probe specific for hsa-miR-181a-5p confirms the upregulation of this miRNA in FTSJ1 loss of function condition already detected by small RNAseq analysis. Above is shown the northern blot after exposition - the whole scan of the blot was converted to Black and White and the saturation was adjusted for the whole image (original exposure is provided in figure. S2d). A ^{32}P-labelled probe specific for human U6 RNA was used to assess equal loading on the blot. Australian and French LCLs point to the country of origin of the LCLs.

FTSJ1 loss of function deregulates mRNAs steady state level

The miRNA pathway has the ability to regulate gene expression post-transcriptionally through translation inhibition and mRNA degradation (Gebert and MacRae 2019). We thus hypothesized that the miRNAs deregulation observed in the NSXLID patient cells (Figures. 2a, 2c, S2b and S2c) may lead to a deregulation of targeted mRNAs steady state levels. In order to obtain insights into the impact of FTSJ1 loss on gene expression control through miRNA-mediated post-transcriptional gene silencing, we performed a transcriptome analysis in patient and control LCLs. This polyA+ transcripts differential expression analysis shows that FTSJ1 dysfunction led to a significant deregulation of 686 genes (Figures. 3a, S3a and S3b). This relatively low number of deregulated genes is in agreement with a previous report showing 775 genes deregulated in human HeLa cells knock-down for *FTSJ1* (Trzaska et al. 2020) as well as with the 110 mRNAs deregulated in KD of one *Drosophila* ortholog (Angelova and Dimitrova et al. 2020).

#	Symbol	baseMean mutant	baseMean wt	log2FoldChange Mutant_vs_WT	padj	#	Symbol	baseMean mutant	baseMean wt	log2FoldChange Mutant_vs_WT	padj
1	SASH1	1002,73	7,65	7,33	2,69E-41	36	RNASE6	639,96	1645,30	-1,72	1,43E-07
2	FCRL4	515,44	7,09	6,05	2,08E-26	37	CD38	3629,12	297,01	2,52	1,60E-07
3	GSTT1	381,66	1,49	8,82	1,81E-18	38	LOC728640	2914,46	2322,11	0,80	2,04E-07
4	PPP1R21	5078,43	6380,13	-1,06	1,92E-17	39	APBB2	1332,24	3371,16	-2,21	2,18E-07
5	TINAG	522,56	2,62	7,59	5,23E-17	40	USMG5	7566,88	6750,46	0,76	2,45E-07
6	ADCY6	544,04	17,61	3,38	1,20E-16	41	FBN2	638,23	76,83	3,67	2,64E-07
7	DSC2	990,21	134,24	3,01	9,55E-15	42	HTR7	2,11	273,06	-21,67	3,12E-07
8	IL17RB	3188,28	616,47	3,45	1,22E-14	43	ALOX5	1890,29	5091,55	-2,91	3,96E-07
9	ABCA12	1267,89	3695,42	-3,75	1,49E-14	44	DDX60L	962,23	110,32	2,42	5,75E-07
10	JAZF1	333,25	17,53	5,14	1,99E-14	45	B3GALNT1	617,28	26,67	4,51	8,73E-07
11	TNRC6C	1612,67	274,90	2,90	3,30E-14	46	COX7B	12243,87	9892,47	0,64	1,05E-06
12	SYNE1	4579,60	5860,78	-0,97	2,35E-13	47	CBLB	3203,88	5817,18	-1,72	1,33E-06
13	CPXM1	2071,71	6,69	8,34	2,34E-12	48	PAPLN	1212,67	3785,94	-1,77	1,35E-06
14	FNIP2	787,53	60,32	2,80	8,93E-12	49	ANKRD26P 3	561,85	2,58	8,71	1,79E-06
15	CDH2	1169,70	45,93	5,50	1,06E-10	50	ACVR2B	355,06	771,16	-1,78	1,88E-06
16	TBX15	2674,86	22,11	5,58	1,52E-10	51	RBPMS	341,58	0,52	8,65	2,01E-06
17	C14orf105	2783,34	168,09	3,35	4,51E-10	52	PSMD7	34420,17	28659,74	0,64	2,07E-06
18	AMPD3	1793,58	4186,29	-2,29	5,50E-10	53	MPHOSPH8	33819,66	28333,28	0,63	2,38E-06
19	GAS2	2013,39	25,82	5,45	7,09E-10	54	CTSW	110,71	8,47	5,36	2,71E-06
20	EVC	293,08	3187,02	-6,61	7,09E-10	55	MYO9B	10534,78	14242,52	-0,53	2,84E-06
21	TNFAIP2	1331,48	3608,85	-1,82	1,15E-09	56	IQGAP2	6537,41	9197,51	-1,20	3,22E-06
22	TSPYL5	829,00	72,33	3,10	1,19E-09	57	AMOTL1	2535,84	68,85	3,67	3,94E-06
23	HERC5	11068,07	2191,72	1,45	1,98E-09	58	MANEAL	354,94	982,06	-1,69	4,72E-06
24	UBE2QL1	205,44	53,77	3,16	2,23E-09	59	SPATS2L	7329,68	2990,72	0,97	4,97E-06
25	ARHGAP6	3915,43	352,19	3,53	2,73E-09	60	VEGFB	6472,65	5415,88	0,90	5,21E-06
26	SLAIN1	6757,48	3157,85	1,24	2,73E-09	61	ATP1B1	7552,46	859,00	2,47	5,25E-06
27	CERS6	5027,25	5425,85	-1,13	3,74E-09	62	SIX3	800,36	1203,65	-6,36	5,25E-06
28	ATP8B1	296,62	13,02	3,73	5,99E-09	63	LOC285972	1639,86	2658,04	-1,16	7,04E-06
29	GRIA3	43,74	504,25	-3,95	7,66E-09	64	MYO18A	8284,31	9316,46	-0,69	8,77E-06
30	MARCH8	1078,97	1225,73	-1,64	7,68E-09	65	L1TD1	67,03	1,01	8,23	8,90E-06
31	DUSP4	17734,90	5898,88	1,94	1,58E-08	66	RRP7B	3521,07	2614,81	0,94	9,80E-06
32	EPB41L5	1929,07	494,79	1,93	1,70E-08	67	SPARC	4705,62	16484,18	-1,60	1,51E-05
33	ZNF711	1265,24	3592,15	-3,34	1,05E-07	68	ESF1	32558,55	26226,19	0,69	1,60E-05
34	RGS2	1264,73	83,46	3,85	1,26E-07	69	FUT8	10906,46	16945,75	-0,94	1,64E-05
35	TP53BP2	2231,99	622,32	2,13	1,41E-07	70	MIR363	109,28	0,00	8,71	1,71E-05

Figure 3a. FTSJ1 loss of function leads to mRNAs deregulation in NSXLID patients LCLs. A list of the 70 most significantly deregulated mRNAs in FTSJ1 LCLs mutants versus controls. The *SPARC* gene at position 67 is highlighted in blue.

Strikingly and even though LCLs do not have a neural origin, analysis of the genes deregulated in patients revealed a clear enrichment (FE =7.9 with raw *p*-value =7.44E-06 and FDR =4.40E-03) in biological process Gene Ontology (GO) term corresponding to brain morphogenesis (Figure. 3b). In addition, and similarly to what we reported in a previous mRNAseq of *Drosophila* S2 cells knocked-down for FTSJ1 ortholog Trm7_34 (Angelova and Dimitrova et al. 2020), 5 out of the top 10 most enriched terms are related to mitochondrial biological processes. In agreement with a recently described role of human FTSJ1 in translational control (Trzaska et al. 2020) and of yeast Trm7 in the general amino-acid control pathway (Han et al. 2018), four biological processes related to translation were affected in FTSJ1 mutated LCLs (FE >3.5, Figure. 3b).

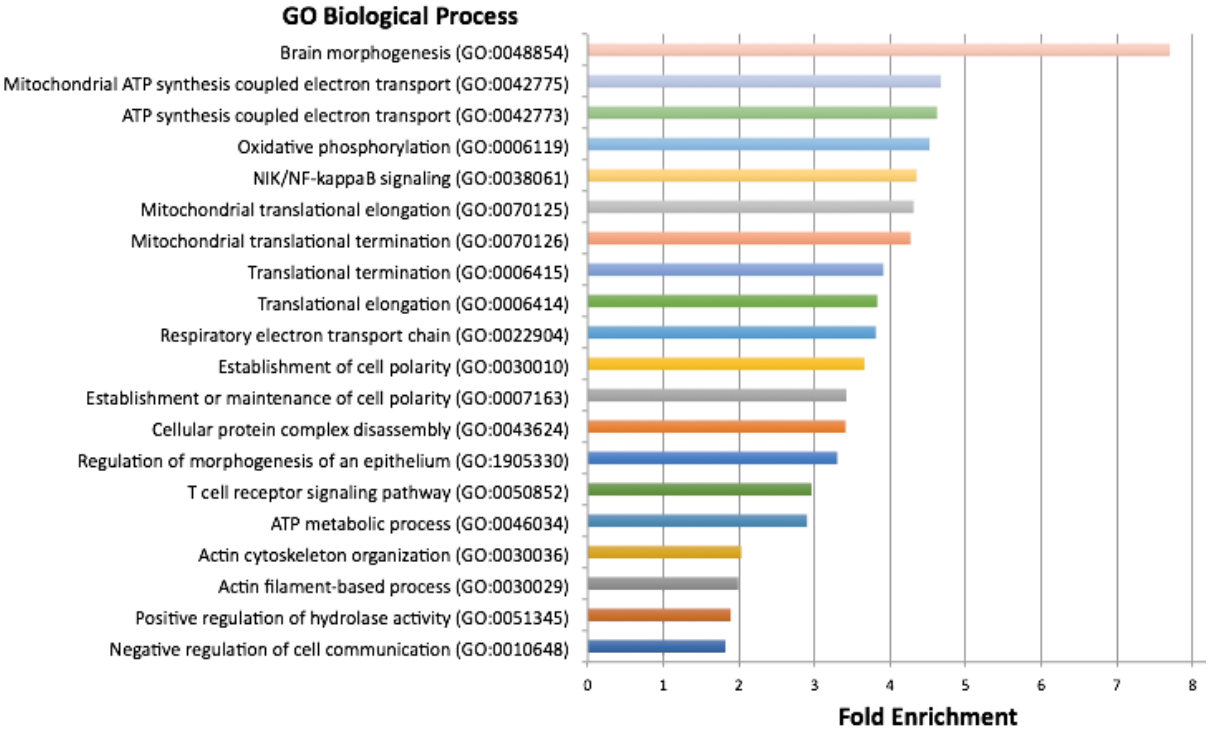

Figure 3b. FTSJ1 loss of function mRNAs GO term. GO analysis of the 686 deregulated genes in FTSJ1 function-deficient LCLs derived from NSXLID patients. The most enriched GO term is Brain morphogenesis. GO analysis was performed using http://geneontology.org/.

As FTSJ1 mutated LCLs originated from patients affected by NSXLID and regarding the recent link of FTSJ1 implication in cancer control pathways (Holzer et al. 2019; Q. He et al. 2020) and the cancer related miRNAs deregulated in patients' LCLs (Figure. 2b), we selected representative and disease-relevant deregulated mRNAs obtained in the RNAseq analysis based on their fold change level of expression and related involvement in brain or cancer diseases.

BTBD3 activity is known to direct the dendritic field orientation during development of the sensory neuron in mice cortex (Matsui et al. 2013) and to regulate mice behaviours (Thompson et al. 2019). Both neuron morphology (Chen et al. 2020) and behaviour (Jensen et al. 2019) were already reported to be affected in intellectual disability patients or mice model of ID, including FTSJ1 KO mice for the latest. Strikingly, *BTBD3* mRNA showed a significantly upregulated steady state level in both mRNAseq (Figure. 3a) and RT-qPCR analysis (Figure. 3c).

SPARC gene product activity was proposed to be involved in both metastasis and tumour suppression (Tai and Tang 2008; Holzer et al. 2019; Q. He et al. 2020). We also investigated the *SPARC* mRNA steady state level in control and mutated FTSJ1 LCLs. *SPARC* mRNA showed a significantly downregulated steady state level in FTSJ1 mutant LCLs when compared to control in both RNAseq and RT-qPCR experiments (Figures. 3a and 3c).

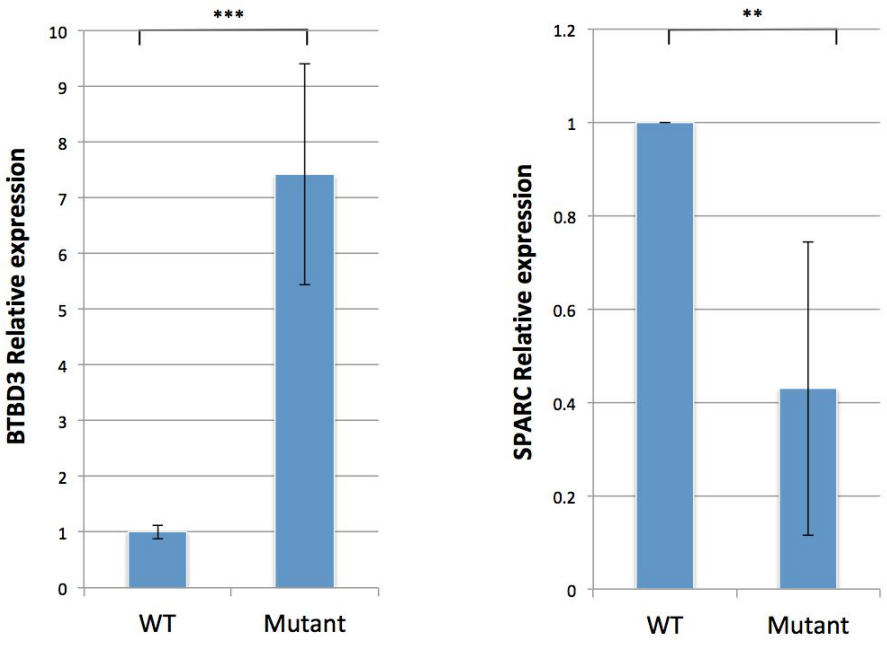

Figure 3c. FTSJ1 loss of function leads to mRNAs deregulation in NSXLID patients LCLs. RT-qPCR analysis confirms deregulation in *BTBD3* and *SPARC* mRNAs expression levels. Normalized to *GAPDH* steady state levels. n=3. *p-values* were calculated with paired Student's *t*-test ***p*=2,58 E-03, ****p*=6,8 E-07. WT values: mean of 2 control FTJS1 LCL. Mutant values: mean of all (x5) *FTSJ1* mutant LCLs of this study.

Taken together, these results are showing a deregulation of certain mRNAs when FTSJ1 activity is lost in patients' blood derived LCLs. Interestingly, as shown for the miRNA small RNAseq analysis (Figure. 2a), several deregulated genes in FTSJ1 mutated LCLs have been linked to cancer and brain functioning.

FTSJ1 deregulated miRNAs target FTSJ1 deregulated mRNAs

As some of the FTSJ1 deregulated miRNAs and mRNAs are implicated in similar biological processes such as cancer and brain function, we wondered if there is some miRNA::mRNA couple that could explain these commonly deregulated processes.

Using miRNet 2.0, we performed a bioinformatics cross-analysis of the small RNAseq and the mRNAseq data analysis. We found a subset of the FTSJ1 deregulated miRNAs for which there is experimental evidence for interacting with some of the FTSJ1 deregulated mRNAs. This cross-analysis showed that the *SPARC* mRNA (down-regulated in FTSJ1 mutated LCLs compared to controls, Figures. 3a and 3c) is a potential target of *mir-10a-5p* (upregulated in FTSJ1 mutated LCLs when compared to healthy individuals, (Figure. 2a)). This observation suggests that *SPARC* mRNA downregulation observed in FTSJ1 mutants could be due to its increased silencing by the upregulated *miR-10a-5p* in FTSJ1-lacking patient cells. Importantly, experimental evidence already showed that *miR-10a* is regulating *SPARC* mRNA steady state level and *SPARC* mRNA possesses permissively identified *miR-10a* binding sites (Bryant et al. 2012; Wang et al. 2020). Intriguingly, the cross-analysis also revealed that the *BTBD3* gene is potentially targeted by *miR-181a-5p (S. He et al. 2015)*, the two of which were upregulated in NSXLID patients-derived LCLs (Figures. 2a, 2c and 3c), implicating a possible connexion between them that differs from the canonical miRNA silencing pathway.

DISCUSSION

In this study, we performed RiboMethSeq on LCL from five individuals with NSXLID caused by a loss of function variants in *FTSJ1 vs.* LCL from four control individuals. RiboMethSeq is a site-specific and unbiased approach to detect Nm modification on tRNAs. First, the technique is performed on total RNA extracts without any sequence specific tRNA purification step implying specific DNA oligonucleotides, which could lead to contaminations with other tRNAs carrying a close nucleotide sequence as well as the extremely abundant 2'-O-modified rRNAs. Second, with RiboMethSeq we can analyse the Nm status of the totality of tRNA species in the human cells and not only selected tRNAs with criteria based on the current but incomplete FTSJ1 targets. Further, RiboMethSeq mapps tRNA reads to the whole tRNA-ome and thus, can identify variations in Nm with single nucleotide resolution. In contrast, mass spectrometry based approaches, although very powerful and sensitive, require the hydrolysis of the tested tRNA into short fragments or single nucleotides, thus the information for the position of these nucleotides in the whole molecule is lost. Indeed, in order to recover the exact position of the modified nucleotides, MS approaches count on the available knowledge of specific tRNAs sequences and modification profiles, listed in RNA modification databases. Unfortunately the latter are not necessarily exhaustive yet as evidence for new modified RNA positions continue to appear regularly in several model organisms, including in human cells.

Importantly, our results from the RiboMethSeq performed on patient and control LCLs confirmed the already known human tRNA targets of FTSJ1. Cm_{32} and Cm_{34} of $tRNA^{Trp(CCA)}$ and position 34 in $tRNA^{Phe(GAA)}$ and $tRNA^{Leu(CAG)}$ were confirmed and we uncovered new FTSJ1 targets not described yet in human samples. Unfortunately, Cm_{32} of $tRNA^{Phe(GAA)}$, which is a well known target of FTSJ1, made an exception and no MethScore variations for position Cm_{32} between control LCL and LCL mutant for FTSJ1 were detected in $tRNA^{Phe}$. The analysis of this position was challenging due to low read numbers necessary for its quantification. FTSJ1 protein deposited Nm at both 32 and 34 positions in $tRNA^{Phe}$, thus the calculated MethScore at position 32 is affected when position 34 of the same tRNA is also Nm modified. Indeed, depicted MethScores (Figure. 1b) were calculated for two neighboring nucleotides (Marchand et al. 2016a). Importantly, raw reads profil inspection shows that Nm at position 32 is lost in FTSJ1 mutated cells when compared to control LCL (Figure. S1b). Finally, we previously reported that $tRNA^{Phe(GAA)}$ ACL positions are challenging to detect with RiboMethSeq, also due to the very specific hyper-modification on position 37 of $tRNA^{Phe}$ (Angelova and Dimitrova et al. 2020). Indeed, $o2yW_{37}$/ m^1G_{37} impairs reverse transcription thereby reducing the number of cDNAs spanning the ACL. Also, we found no variations in MehtScore of Cm_{34} in $tRNA^{Leu(CAA)}$, which is probably due to a low read number

considering that this target was previously reported in human cell culture (Kawarada et al. 2017) and in flies (Angelova and Dimitrova et al. 2020). Again, the reason may be the hyper-modified nature of this nucleotide position (f^5C34/hm^5C34 before methylation by FTSJ1 (Kawarada et al. 2017)) which may have interfered with the random hydrolysis of the RiboMethSeq and/or the reverse transcription steps. However, we detected a FTSJ1-dependent Nm on C_{34} of another $tRNA^{Leu}$ isoacceptor: $tRNA^{Leu(CAG)}$ which was recently confirmed by another study performed in HEK293T human cells (Jing Li et al. 2020).

Finally and importantly, we were able to uncover novel and unexpected tRNA targets for FTSJ1: Cm_{32} $tRNA^{Arg(UCG)}$, Cm_{32} $tRNA^{Gln(CUG)}$ and Um_{32} $tRNA^{Gly(CCC)}$. In the case of $tRNA^{Arg(UCG)}$ it seems that we uncovered not only a new target for FTSJ1, but also an unknown modification as Cm_{32} was reported on modomics database only for two other isoacceptors ($tRNA^{Arg(CCU)}$ and $tRNA^{Arg(UCU)}$) and not for $tRNA^{Arg(UCG)}$ (Boccaletto et al. 2018). Similarly, there was no evidence for a human Cm_{32} $tRNA^{Gln(CUG)}$ and only the other isoacceptor $tRNA^{Gln(UUG)}$ was reported in Modomics as 2'-O-methylated at C_{32}. Still, Cm_{32} on $tRNA^{Gln(CUG)}$ was recently discovered as a target of *Drosophila* Trm7_32 (Angelova and Dimitrova et al. 2020). Among the newly uncovered FTSJ1 targets in this study, Um_{32} $tRNA^{Gly(CCC)}$ was the only one that has been reported in Modomics, however the enzyme responsible for this modification was unknown. Our results point to FTSJ1 as one of the dedicated Nm-Mtase that modified U at position 32 on $tRNA^{Gly(CCC)}$.

During the course of our study, a new study performed on HEK293T CRISPR FTSJ1 mutant used UPLC-MS/MS and revealed tRNA targets for FTSJ1 after purifying a subset of selected tRNAs (Jing Li et al. 2020). The results of this study are similar to our RiboMethSeq approach, however we report here some differences and, importantly, in samples originating from patients' blood. The UPLC-MS/MS confirms the targeting of Cm_{32} $tRNA^{Arg(UCG)}$ by FTSJ1, as revealed by our RiboMethSeq, but also detects FTSJ1-dependent Cm_{32} $tRNA^{Arg(ACG)}$ and Um_{32} and Cm_{34} $tRNA^{Arg(CCG)}$. In the case of Cm_{34} $tRNA^{Arg(CCG)}$, the authors of the study assume that it may be a false positive due to a possible contamination by another isodecoder $tRNA^{Arg(CCG)-2-1}$ which has C_{32} and high sequence similarity with $tRNA^{Arg(CCG)}$ (Maraia and Arimbasseri 2017; Jing Li et al. 2020). Thus the observed change on Cm_{34} $tRNA^{Arg(CCG)}$ in FTSJ1 KO HEK293T cells may come from Cm_{32} of $tRNA^{Arg(CCG)-2-1}$ that seems to be modified by FTSJ1. This example highlights one of the limitations of UPLC-MS/MS when compared to RiboMethSeq. The study by (Jing Li et al. 2020) confirmed our results on Cm_{34} $tRNA^{Leu(CAG)}$, but did not test Um_{32} $tRNA^{Gly(CCC)}$, nor Cm_{32} $tRNA^{Gln(CUG)}$, instead however they identified a FTSJ1-dependent Cm_{32} $tRNA^{Gln(UUG)}$.

As discussed above, it is important to note that UPLC-MS/MS studies could be biased in their way of identifying the Nm sites mostly during the selection step and potential contaminations of the purified tested tRNAs by other similar in sequence tRNAs as well as

the heavily Nm-modified rRNAs. Similarly, for specific and identified hyper-modified tRNA positions as mentioned for $tRNA^{Phe(GAA)}$ and on Cm_{34} of $tRNA^{Leu(CAA)}$, RiboMethSeq showed also its limitations. Thus, even regarding the strong effort realised by several teams the last 5 years to identify precisely Nm modification on mammalian tRNA, we do not exclude the possibility that there may still be other tRNA targets of FTSJ1 that were not uncovered yet neither by MS nor by RiboMethSeq approaches. This is why we believe that a combinatorial approach is of great interest in the future for the community as well as ongoing approaches to detect Nm modification using direct RNA sequencing nanopore approach (Ueda 2020). Importantly, our RiboMethSeq results performed on NSXLID patients' blood-derived LCLs have with confidence extended the panel of FTSJ1's tRNA targets, thus providing new potential biomarker sources for diagnosis of FTSJ1-related intellectual disability in the future.

Another major goal of this study was to test if the sncRNA deregulation phenotype reported in flies lacking FTSJ1 homologues (Angelova and Dimitrova et al. 2020) is conserved in human cells lacking FTSJ1 activity. We thus decided to evaluate the miRNA populations of these cells through next generation sequencing by performing small RNAseq. Consistently with the well known FTSJ1 implication in ID and more recently in cancer (Holzer et al. 2019; Q. He et al. 2020), we found 36 differentially expressed miRNAs, most of which were already associated with brain diseases and functioning and/or cancer development. The most prevalent associated cancer types were the ones related to the brain tissues. Consistently with the post-transcription regulation role of miRNA, we also found through mRNAseq an enrichment of brain morphogenesis-related mRNAs differentially expressed in FTSJ1 loss of function when compared to control LCLs. Strikingly, a cross-analysis of these two RNA sequencing experiments revealed potential miRNA::target mRNA couples among the deregulated RNA populations. This is indicative of possible miRNA silencing changes in the absence of FTSJ1, similarly to what we report earlier in *Drosophila* FTSJ1 mutants orthologs. The predicted miRNA::mRNA couples need to be further validated individually in neuronal tissues, although they were reported from miRnet database (https://www.mirnet.ca/) that already includes experimental evidence on the miRNA::mRNA regulation, particularly for *BTBD3* and *SPARC* mRNAs (Bryant et al. 2012; Wang et al. 2020; S. He et al. 2015).

We previously showed that mRNAseq in *Trm7_34* KD *Drosophila* S2 cells revealed that 8 out of the top 10 differentially expressed genes compared to controls were related to mitochondria (*e.g.*, NADH dehydrogenases, cytochrome-c oxidases, ATPase6 and others (Angelova and Dimitrova et al. 2020)). Strikingly, the Gene Ontology analysis on mRNAseq from human LCLs showed similarly an enrichment of mitochondrion-related biological

processes GO terms (*e.g.* ATP synthesis coupled electron transport, oxidative phosphorylation, mitochondrial translation) among the differentially expressed genes in the FTSJ1-deficient LCLs. Considering the huge energy demands of the brain, it seems logical that a deregulation in mitochondrial energy metabolism cause brain malfunctioning including reported developmental intellectual issues (Hara et al. 2014; Picard and McEwen 2014; Guevara-Campos, González-Guevara, and Cauli 2015; Valiente-Pallejà et al. 2018). Importantly, alteration in energy metabolisms in *FTSJ1* depleted cells was previously reported in *Ftsj1* KO mice that also present behavioural phenotypes similar to human ID patients (memory and learning troubles (Jensen et al. 2019)).

The development of companion diagnostics in addition to the exome-sequencing approaches used in human genetics disease diagnosis is increasing the efficiency, time and cost-benefit detection of gene mutation provoking disease such as ID in humans. Interestingly, in this study we identify *miR-181a-5p* as a potential human biomarker of FTSJ1 activity. Fortunately, this study was performed on LCLs that are derived from the blood of patients and *miR-181a-5p* is reported to be circulant in human bloodstream (Magen et al. 2019). Thus, in the longer term, we hope to characterize accumulation of *miR-181a-5p* in crude blood samples or plasma cell-free of ID patients carrying a *FTSJ1* mutation to facilitate the diagnosis of ID-FTSJ1 patients. The heterogeneity of ID makes it extremely challenging for genetic and clinical diagnosis (Ilyas et al. 2020). The power of such circulant RNA biomarkers as *miR-181a-5p* is, whatever the reason of the faulty FTSJ1 protein activity (genetics, epigenetics, environmental), the observation of abnormally abundant *miR-181a-5p* in FTSJ1 patients blood cells will lead to the conclusion that FTSJ1 activity is compromised. Such “functional companion diagnostic” will help for earlier and accurate detection of faulty FTSJ1 activity, in particular for FTSJ1 variants that give rise to hardly predictable pathological protein activity (missense mutations such LCL22 in this study).

Importantly, several RNAs are stable and longly detectable in human bloodstream (Umu et al. 2018; Galvanin et al. 2019), indeed some of these circulating and stable RNAs are already used to challenge the effectiveness of patient treatment (Guo et al. 2015). These observations highlight the usefulness of companion diagnostics in clinical settings that would become solid diagnostic and prognostic markers in the future.

ACKNOWLEDGMENTS

The authors thank the patients and their families for their participation in the study. The authors also want to thank Christelle Thibaut-Charpentier from the GenomEast sequencing platform in Strasbourg, a member of the 'France Génomique' consortium (ANR-10-INBS-0009), the Institut de Génétique Médicale d'Alsace for their technical support and Myriam Bronner from Nancy University Hospital for the establishment of the LCL-MM line. C.C. received financial support from the CNRS, Sorbonne Université, the Fondation Maladies Rares (Genomics-2018 #11809), the IBPS-2020 Action Incitative and the Ligue National contre le cancer Île de France (RS21/76-29) and thanks them for their support. We would like to thank the members of the *TErBio* laboratory for helpful discussions and reading of the manuscript. Y.M. and C.C. are members of the European EPITRAN COST Action (CA16120) and thanks them for their support. D.G.D. and M.B. have PhD fellowships from the Ministère de la Recherche et de l'Enseignement Supérieur at the doctoral school Complexité du Vivant (ED515). We also thank the Fondation ARC pour la Recherche sur le Cancer for funding support to D.G.D. 4th year PhD; 'Réseau André Picard', the 'Société Française de Génétique' (to M.B. and D.G.D.) and COST action 'EPITRAN' CA16120 (to Y.M., V.M., D.G.D., M.B. and C.C.) for traveling fellowship grants.

REFERENCES

Abe, Masashi, Ammar Naqvi, Gert-Jan Hendriks, Virzhiniya Feltzin, Yongqing Zhu, Andrey Grigoriev, and Nancy M. Bonini. 2014. "Impact of Age-Associated Increase in 2′-O-Methylation of miRNAs on Aging and Neurodegeneration in Drosophila." *Genes & Development* 28 (1): 44–57.

Angelova, Margarita T., Dilyana G. Dimitrova, Bruno Da Silva, Virginie Marchand, Caroline Jacquier, Cyrinne Achour, Mira Brazane, et al. 2020. "tRNA 2′-O-Methylation by a Duo of TRM7/FTSJ1 Proteins Modulates Small RNA Silencing in Drosophila." *Nucleic Acids Research* 48 (4): 2050–72.

Angelova, Margarita T., Dilyana G. Dimitrova, Nadja Dinges, Tina Lence, Lina Worpenberg, Clément Carré, and Jean-Yves Roignant. 2018. "The Emerging Field of Epitranscriptomics in Neurodevelopmental and Neuronal Disorders." *Frontiers in Bioengineering and Biotechnology* 6 (April): 46.

Birkedal, Ulf, Mikkel Christensen-Dalsgaard, Nicolai Krogh, Radhakrishnan Sabarinathan, Jan Gorodkin, and Henrik Nielsen. 2015. "Profiling of Ribose Methylations in RNA by High-Throughput Sequencing." *Angewandte Chemie* 54 (2): 451–55.

Boccaletto, Pietro, Magdalena A. Machnicka, Elzbieta Purta, Pawel Piatkowski, Blazej Baginski, Tomasz K. Wirecki, Valérie de Crécy-Lagard, et al. 2018. "MODOMICS: A Database of RNA Modification Pathways. 2017 Update." *Nucleic Acids Research* 46 (D1): D303–7.

Bolger, Anthony M., Marc Lohse, and Bjoern Usadel. 2014. "Trimmomatic: A Flexible Trimmer for Illumina Sequence Data." *Bioinformatics* 30 (15): 2114–20.

Bryant, Adam, Catalina A. Palma, Vivek Jayaswal, Yee Wa Yang, Mark Lutherborrow, and David Df Ma. 2012. "miR-10a Is Aberrantly Overexpressed in Nucleophosmin1 Mutated Acute Myeloid Leukaemia and Its Suppression Induces Cell Death." *Molecular Cancer* 11 (February): 8.

Bügl, H., E. B. Fauman, B. L. Staker, F. Zheng, S. R. Kushner, M. A. Saper, J. C. Bardwell, and U. Jakob. 2000. "RNA Methylation under Heat Shock Control." *Molecular Cell* 6 (2): 349–60.

Cavaillé, Jérôme. 2017. "Box C/D Small Nucleolar RNA Genes and the Prader-Willi Syndrome: A Complex Interplay." *Wiley Interdisciplinary Reviews. RNA* 8 (4). https://doi.org/10.1002/wrna.1417.

Chan, Patricia P., and Todd M. Lowe. 2016. "GtRNAdb 2.0: An Expanded Database of Transfer RNA Genes Identified in Complete and Draft Genomes." *Nucleic Acids Research* 44 (D1): D184–89.

Chen, J., M. E. Lambo, G. Xia, J. T. Dearborn, and Y. Liu. 2020. "A MYT1L Syndrome Mouse Model Recapitulates Patient Phenotypes and Reveals Altered Brain Development due to Disrupted Neuronal Maturation." *bioRxiv*. https://www.biorxiv.org/content/10.1101/2020.12.17.423095v1.abstract.

Conti, Alfredo, Sara G. Romeo, Annamaria Cama, Domenico La Torre, Valeria Barresi, Gaetana Pezzino, Chiara Tomasello, et al. 2016. "MiRNA Expression Profiling in Human Gliomas: Upregulated miR-363 Increases Cell Survival and Proliferation." *Tumour Biology: The Journal of the International Society for Oncodevelopmental Biology and Medicine*

37 (10): 14035–48.

Dai, Qing, Sharon Moshitch-Moshkovitz, Dali Han, Nitzan Kol, Ninette Amariglio, Gideon Rechavi, Dan Dominissini, and Chuan He. 2017. “Nm-Seq Maps 2′-O-Methylation Sites in Human mRNA with Base Precision.” *Nature Methods*. https://doi.org/10.1038/nmeth.4294.

Darzacq, X. 2002. “Cajal Body-Specific Small Nuclear RNAs: A Novel Class of 2’-O-Methylation and Pseudouridylation Guide RNAs.” *The EMBO Journal*. https://doi.org/10.1093/emboj/21.11.2746.

Dimitrova, Dilyana G., Laure Teysset, and Clément Carré. 2019. “RNA 2’-O-Methylation (Nm) Modification in Human Diseases.” *Genes* 10 (2). https://doi.org/10.3390/genes10020117.

Ding, Haixia, Zhen Huang, Mengjie Chen, Cheng Wang, Xi Chen, Jiangning Chen, and Junfeng Zhang. 2016. “Identification of a Panel of Five Serum miRNAs as a Biomarker for Parkinson’s Disease.” *Parkinsonism & Related Disorders* 22 (January): 68–73.

Dostie, Josée, Zissimos Mourelatos, Michael Yang, Anup Sharma, and Gideon Dreyfuss. 2003. “Numerous microRNPs in Neuronal Cells Containing Novel microRNAs.” *RNA* 9 (2): 180–86.

El Hassouni, Btissame, Dzjemma Sarkisjan, J. Chris Vos, Elisa Giovannetti, and Godefridus J. Peters. 2019. “Targeting the Ribosome Biogenesis Key Molecule Fibrillarin to Avoid Chemoresistance.” *Current Medicinal Chemistry* 26 (33): 6020–32.

Erales, Jenny, Virginie Marchand, Baptiste Panthu, Sandra Gillot, Stéphane Belin, Sandra E. Ghayad, Maxime Garcia, et al. 2017. “Evidence for rRNA 2′-O-Methylation Plasticity: Control of Intrinsic Translational Capabilities of Human Ribosomes.” *Proceedings of the National Academy of Sciences of the United States of America* 114 (49): 12934–39.

Feder, Marcin, Jakub Pas, Lucjan S. Wyrwicz, and Janusz M. Bujnicki. 2003. “Molecular Phylogenetics of the RrmJ/fibrillarin Superfamily of Ribose 2’-O-Methyltransferases.” *Gene* 302 (1-2): 129–38.

Freude, Kristine, Kirsten Hoffmann, Lars-Riff Jensen, Martin B. Delatycki, Vincent des Portes, Bettina Moser, Ben Hamel, et al. 2004. “Mutations in the FTSJ1 Gene Coding for a Novel S-Adenosylmethionine–Binding Protein Cause Nonsyndromic X-Linked Mental Retardation.” *American Journal of Human Genetics* 75 (2): 305–9.

Froyen, Guy, Marijke Bauters, Jackie Boyle, Hilde Van Esch, Karen Govaerts, Hans van Bokhoven, Hans-Hilger Ropers, et al. 2007. “Loss of SLC38A5 and FTSJ1 at Xp11.23 in Three Brothers with Non-Syndromic Mental Retardation due to a Microdeletion in an Unstable Genomic Region.” *Human Genetics* 121 (5): 539–47.

Galvanin, Adeline, Gabriel Dostert, Lilia Ayadi, Virginie Marchand, Émilie Velot, and Yuri Motorin. 2019. “Diversity and Heterogeneity of Extracellular RNA in Human Plasma.” *Biochimie* 164 (September): 22–36.

Gebert, Luca F. R., and Ian J. MacRae. 2019. “Regulation of microRNA Function in Animals.” *Nature Reviews. Molecular Cell Biology* 20 (1): 21–37.

Gillies, Jana K., and Ian A. J. Lorimer. 2007. “Regulation of p27Kip1 by miRNA 221/222 in Glioblastoma.” *Cell Cycle* 6 (16): 2005–9.

Guevara-Campos, José, Lucía González-Guevara, and Omar Cauli. 2015. “Autism and Intellectual Disability Associated with Mitochondrial Disease and Hyperlactacidemia.” *International Journal of Molecular Sciences* 16 (2): 3870–84.

Guo, Yan, Amma Bosompem, Sanjay Mohan, Begum Erdogan, Fei Ye, Kasey C. Vickers, Quanhu Sheng, et al. 2015. “Transfer RNA Detection by Small RNA Deep Sequencing and Disease Association with Myelodysplastic Syndromes.” *BMC Genomics* 16 (September): 727.

Guy, Michael P., and Eric M. Phizicky. 2015. “Conservation of an Intricate Circuit for Crucial Modifications of the tRNAPhe Anticodon Loop in Eukaryotes.” *RNA* 21 (1): 61–74.

Guy, Michael P., Brandon M. Podyma, Melanie A. Preston, Hussam H. Shaheen, Kady L. Krivos, Patrick A. Limbach, Anita K. Hopper, and Eric M. Phizicky. 2012. “Yeast Trm7 Interacts with Distinct Proteins for Critical Modifications of the tRNAPhe Anticodon Loop.” *RNA* 18 (10): 1921–33.

Guy, Michael P., Marie Shaw, Catherine L. Weiner, Lynne Hobson, Zornitza Stark, Katherine Rose, Vera M. Kalscheuer, Jozef Gecz, and Eric M. Phizicky. 2015. “Defects in tRNA Anticodon Loop 2’-O-Methylation Are Implicated in Nonsyndromic X-Linked Intellectual Disability due to Mutations in FTSJ1.” *Human Mutation* 36 (12): 1176–87.

Han, Lu, Michael P. Guy, Yoshiko Kon, and Eric M. Phizicky. 2018. “Lack of 2’-O-Methylation in the tRNA Anticodon Loop of Two Phylogenetically Distant Yeast Species Activates the General Amino Acid Control Pathway.” *PLoS Genetics* 14 (3): e1007288.

Hara, Yuko, Frank Yuk, Rishi Puri, William G. M. Janssen, Peter R. Rapp, and John H. Morrison. 2014. “Presynaptic Mitochondrial Morphology in Monkey Prefrontal Cortex Correlates with Working Memory and Is Improved with Estrogen Treatment.” *Proceedings of the National Academy of Sciences of the United States of America* 111 (1): 486–91.

He, Qihan, Lin Yang, Kaiping Gao, Peikun Ding, Qianqian Chen, Juan Xiong, Wenhan Yang, et al. 2020. “FTSJ1 Regulates tRNA 2′-O-Methyladenosine Modification and Suppresses the Malignancy of NSCLC via Inhibiting DRAM1 Expression.” *Cell Death & Disease* 11 (5): 1–12.

He, Shuming, Shumei Zeng, Zhi-Wei Zhou, Zhi-Xu He, and Shu-Feng Zhou. 2015. “Hsa-microRNA-181a Is a Regulator of a Number of Cancer Genes and a Biomarker for Endometrial Carcinoma in Patients: A Bioinformatic and Clinical Study and the Therapeutic Implication.” *Drug Design, Development and Therapy* 9 (February): 1103–75.

Holzer, Kerstin, Alessandro Ori, Amy Cooke, Daniel Dauch, Elisabeth Drucker, Philip Riemenschneider, Amparo Andres-Pons, et al. 2019. “Nucleoporin Nup155 Is Part of the p53 Network in Liver Cancer.” *Nature Communications* 10 (1): 2147.

Horwich, Michael D., Chengjian Li, Christian Matranga, Vasily Vagin, Gwen Farley, Peng Wang, and Phillip D. Zamore. 2007. “The Drosophila RNA Methyltransferase, DmHen1, Modifies Germline piRNAs and Single-Stranded siRNAs in RISC.” *Current Biology: CB* 17 (14): 1265–72.

Ilyas, Muhammad, Asif Mir, Stephanie Efthymiou, and Henry Houlden. 2020. “The Genetics of Intellectual Disability: Advancing Technology and Gene Editing.” *F1000Research* 9 (January). https://doi.org/10.12688/f1000research.16315.1.

Jensen, Lars R., Lillian Garrett, Sabine M. Hölter, Birgit Rathkolb, Ildikó Rácz, Thure Adler, Cornelia Prehn, et al. 2019. “A Mouse Model for Intellectual Disability Caused by Mutations in the X-Linked 2′-O-methyltransferase Ftsj1 Gene.” *Biochimica et Biophysica Acta (BBA) - Molecular Basis of Disease* 1865 (9): 2083–93.

Jiang, Chuanfu, Yang Cao, Ting Lei, Yu Wang, Junfeng Fu, Ze Wang, and Zhenyang Lv. 2018. “microRNA-363-3p Inhibits Cell Growth and Invasion of Non-small Cell Lung Cancer by Targeting HMGA2.” *Molecular Medicine Reports* 17 (2): 2712–18.

Jia, Yichang, John C. Mu, and Susan L. Ackerman. 2012. “Mutation of a U2 snRNA Gene Causes Global Disruption of Alternative Splicing and Neurodegeneration.” *Cell* 148 (1-2): 296–308.

Kawai, Gota, Yuriko Yamamoto, Takashi Kamimura, Tsukio Masegi, Mitsuo Sekine, Tsujiaki Hata, Takamasa Iimori, Tatsuo Watanabe, Tatsuo Miyazawa, and Shigeyuki Yokoyama. 1992. "Conformational Rigidity of Specific Pyrimidine Residues in tRNA Arises from Posttranscriptional Modifications That Enhance Steric Interaction between the Base and the 2'-Hydroxyl Group." *Biochemistry*. https://doi.org/10.1021/bi00119a012.

Kawarada, Layla, Takeo Suzuki, Takayuki Ohira, Shoji Hirata, Kenjyo Miyauchi, and Tsutomu Suzuki. 2017. "ALKBH1 Is an RNA Dioxygenase Responsible for Cytoplasmic and Mitochondrial tRNA Modifications." *Nucleic Acids Research* 45 (12): 7401–15.

Khalil, Alia, Hayfa Medfai, Philippe Poelvoorde, Mohammad Fayyad Kazan, Cedric Delporte, Pierre Van Antwerpen, Yolla EL-Makhour, et al. 2018. "Myeloperoxidase Promotes Tube Formation, Triggers ERK1/2 and Akt Pathways and Is Expressed Endogenously in Endothelial Cells." *Archives of Biochemistry and Biophysics* 654 (September): 55–69.

Khuu, Cuong, Amer Sehic, Lars Eide, and Harald Osmundsen. 2016. "Anti-Proliferative Properties of miR-20b and miR-363 from the miR-106a-363 Cluster on Human Carcinoma Cells." *MicroRNA (Shariqah, United Arab Emirates)* 5 (1): 19–35.

Kretschmann, Anita, Benedicte Danis, Lidija Andonovic, Khalid Abnaof, Marijke van Rikxoort, Franziska Siegel, Manuela Mazzuferi, et al. 2015. "Different microRNA Profiles in Chronic Epilepsy versus Acute Seizure Mouse Models." *Journal of Molecular Neuroscience: MN* 55 (2): 466–79.

Kristen M Bartoli, Cassandra Schaening, Thomas Carlile, Wendy V Gilbert. n.d. "Conserved Methyltransferase Spb1 Targets mRNAs for Regulated Modification with 2′-O-Methyl Ribose." bioRxiv. https://doi.org/10.1101/271916.

Kurth, Henriette M., and Kazufumi Mochizuki. 2009. "2'-O-Methylation Stabilizes Piwi-Associated Small RNAs and Ensures DNA Elimination in Tetrahymena." *RNA* 15 (4): 675–85.

Lacoux, Caroline, Daniele Di Marino, Pietro Pilo Boyl, Francesca Zalfa, Bing Yan, Maria Teresa Ciotti, Mattia Falconi, et al. 2012. "BC1-FMRP Interaction Is Modulated by 2′-O-Methylation: RNA-Binding Activity of the Tudor Domain and Translational Regulation at Synapses." *Nucleic Acids Research*. https://doi.org/10.1093/nar/gkr1254.

Langmead, Ben, and Steven L. Salzberg. 2012. "Fast Gapped-Read Alignment with Bowtie 2." *Nature Methods* 9 (4): 357–59.

Langmead, Ben, Cole Trapnell, Mihai Pop, and Steven L. Salzberg. 2009. "Ultrafast and Memory-Efficient Alignment of Short DNA Sequences to the Human Genome." *Genome Biology* 10 (3): R25.

Lau, Pierre, Koen Bossers, Rekin 's Janky, Evgenia Salta, Carlo Sala Frigerio, Shahar Barbash, Roy Rothman, et al. 2013. "Alteration of the microRNA Network during the Progression of Alzheimer's Disease." *EMBO Molecular Medicine* 5 (10): 1613–34.

Li, Jing, Yan-Nan Wang, Bei-Si Xu, Ya-Ping Liu, Mi Zhou, Tao Long, Hao Li, et al. 2020. "Intellectual Disability-Associated Gene ftsj1 Is Responsible for 2′-O-Methylation of Specific tRNAs." *EMBO Reports*, e50095.

Li, Junjie, Zhiyong Yang, Bin Yu, Jun Liu, and Xuemei Chen. 2005. "Methylation Protects miRNAs and siRNAs from a 3′-End Uridylation Activity in Arabidopsis." *Current Biology: CB* 15 (16): 1501–7.

Liu, Bin, Jing Li, Min Zheng, Jun Ge, Juan Li, and Ping Yu. 2017. "MiR-542-3p Exerts Tumor Suppressive Functions in Non-Small Cell Lung Cancer Cells by Upregulating FTSJ2." *Life Sciences* 188 (November): 87–95.

Li, Yiyi, Cem Kuscu, Anna Banach, Qian Zhang, Ashleigh Pulkoski-Gross, Deborah Kim, Jingxuan Liu, et al. 2015. "miR-181a-5p Inhibits Cancer Cell Migration and Angiogenesis via Downregulation of Matrix Metalloproteinase-14." *Cancer Research* 75 (13): 2674–85.

Love, M. I., W. Huber, and S. Anders. 2014. "Moderated Estimation of Fold Change and Dispersion for RNA-Seq Data with DESeq. 2 Genome Biol 15: 550."

Lund, A. H. 2010. "miR-10 in Development and Cancer." *Cell Death and Differentiation* 17 (2): 209–14.

Magen, Iddo, Anna Coenen-Stass, Nancy S. Yacovzada, Julian Grosskreutz, Ching-Hua Lu, Linda Greensmith, Andrea Malaspina, Pietro Fratta, and Eran Hornstein. 2019. "Circulating miR-181a-5p Is a Prognostic Biomarker for Amyotrophic Lateral Sclerosis." *Cold Spring Harbor Laboratory*. https://doi.org/10.1101/833079.

Maraia, Richard J., and Aneeshkumar G. Arimbasseri. 2017. "Factors That Shape Eukaryotic tRNAomes: Processing, Modification and Anticodon–Codon Use." *Biomolecules* 7 (1): 26.

Marcel, Virginie, Janice Kielbassa, Virginie Marchand, Kundhavai S. Natchiar, Hermes Paraqindes, Flora Nguyen Van Long, Lilia Ayadi, et al. 2020. "Ribosomal RNA 2'O-Methylation as a Novel Layer of Inter-Tumour Heterogeneity in Breast Cancer." *NAR Cancer*. https://doi.org/10.1093/narcan/zcaa036.

Marchand, Virginie, Florence Blanloeil-Oillo, Mark Helm, and Yuri Motorin. 2016a. "Illumina-Based RiboMethSeq Approach for Mapping of 2'-O-Me Residues in RNA." *Nucleic Acids Research* 44 (16): e135.

———. 2016b. "Illumina-Based RiboMethSeq Approach for Mapping of 2'-O-Me Residues in RNA." *Nucleic Acids Research* 44 (16): e135.

Marchand, Virginie, Florian Pichot, Kathrin Thüring, Lilia Ayadi, Isabel Freund, Alexander Dalpke, Mark Helm, and Yuri Motorin. 2017. "Next-Generation Sequencing-Based RiboMethSeq Protocol for Analysis of tRNA 2′-O-Methylation." *Biomolecules* 7 (1): 13.

Matsui, Asuka, May Tran, Aya C. Yoshida, Satomi S. Kikuchi, Mami U, Masaharu Ogawa, and Tomomi Shimogori. 2013. "BTBD3 Controls Dendrite Orientation toward Active Axons in Mammalian Neocortex." *Science* 342 (6162): 1114–18.

Noma, Akiko, Yohei Kirino, Yoshiho Ikeuchi, and Tsutomu Suzuki. 2006. "Biosynthesis of Wybutosine, a Hyper-Modified Nucleoside in Eukaryotic Phenylalanine tRNA." *The EMBO Journal* 25 (10): 2142–54.

Picard, Martin, and Bruce S. McEwen. 2014. "Mitochondria Impact Brain Function and Cognition." *Proceedings of the National Academy of Sciences of the United States of America*.

Pichot, Florian, Virginie Marchand, Lilia Ayadi, Valérie Bourguignon-Igel, Mark Helm, and Yuri Motorin. 2020. "Holistic Optimization of Bioinformatic Analysis Pipeline for Detection and Quantification of 2'-O-Methylations in RNA by RiboMethSeq." *Frontiers in Genetics* 11 (February): 38.

Pintard, Lionel, François Lecointe, Janusz M. Bujnicki, Claire Bonnerot, Henri Grosjean, and Bruno Lapeyre. 2002. "Trm7p Catalyses the Formation of Two 2'-O-Methylriboses in Yeast tRNA Anticodon Loop." *The EMBO Journal* 21 (7): 1811–20.

Quinlan, Aaron R. 2014. "BEDTools: The Swiss-Army Tool for Genome Feature Analysis." *Current Protocols in Bioinformatics / Editoral Board, Andreas D. Baxevanis ... [et Al.]* 47 (September): 11.12.1–34.

Ramser, J., B. Winnepenninckx, C. Lenski, V. Errijgers, M. Platzer, C. E. Schwartz, A. Meindl, and R. F. Kooy. 2004. "A Splice Site Mutation in the Methyltransferase Gene FTSJ1 in Xp11.23 Is Associated with

Non-Syndromic Mental Retardation in a Large Belgian Family (MRX9)." *Journal of Medical Genetics* 41 (9): 679–83.

Roser, Anna Elisa, Lucas Caldi Gomes, Jonas Schünemann, Fabian Maass, and Paul Lingor. 2018. "Circulating miRNAs as Diagnostic Biomarkers for Parkinson's Disease." *Frontiers in Neuroscience* 12 (September): 625.

Saito, Kuniaki, Yuriko Sakaguchi, Takeo Suzuki, Tsutomu Suzuki, Haruhiko Siomi, and Mikiko C. Siomi. 2007. "Pimet, the Drosophila Homolog of HEN1, Mediates 2′-O-Methylation of Piwi- Interacting RNAs at Their 3′ Ends." *Genes & Development* 21 (13): 1603–8.

Saletore, Yogesh, Kate Meyer, Jonas Korlach, Igor D. Vilfan, Samie Jaffrey, and Christopher E. Mason. 2012. "The Birth of the Epitranscriptome: Deciphering the Function of RNA Modifications." *Genome Biology* 13 (10): 175.

Shi, Lei, Zihao Cheng, Junxia Zhang, Rui Li, Peng Zhao, Zhen Fu, and Yongping You. 2008. "Hsa-Mir-181a and Hsa-Mir-181b Function as Tumor Suppressors in Human Glioma Cells." *Brain Research* 1236 (October): 185–93.

Su, Yingxue, Jiani Yuan, Feiran Zhang, Qingqing Lei, Tingting Zhang, Kai Li, Jiawei Guo, et al. 2019. "MicroRNA-181a-5p and microRNA-181a-3p Cooperatively Restrict Vascular Inflammation and Atherosclerosis." *Cell Death & Disease* 10 (5): 365.

Tai, Isabella T., and Michelle J. Tang. 2008. "SPARC in Cancer Biology: Its Role in Cancer Progression and Potential for Therapy." *Drug Resistance Updates: Reviews and Commentaries in Antimicrobial and Anticancer Chemotherapy* 11 (6): 231–46.

Thompson, Summer L., Amanda C. Welch, Emily V. Ho, João M. Bessa, Carlos Portugal-Nunes, Mónica Morais, Jared W. Young, James A. Knowles, and Stephanie C. Dulawa. 2019. "Btbd3 Expression Regulates Compulsive-like and Exploratory Behaviors in Mice." *Translational Psychiatry* 9 (1): 222.

Trzaska, Carole, Séverine Amand, Christine Bailly, Catherine Leroy, Virginie Marchand, Evelyne Duvernois-Berthet, Jean-Michel Saliou, et al. 2020. "2,6-Diaminopurine as a Highly Potent Corrector of UGA Nonsense Mutations." *Nature Communications*. https://doi.org/10.1038/s41467-020-15140-z.

Ueda, H. 2020. "nanoDoc: RNA Modification Detection Using Nanopore Raw Reads with Deep One-Class Classification." *bioRxiv*. https://www.biorxiv.org/content/10.1101/2020.09.13.295089v1.abstract.

Umu, Sinan Uğur, Hilde Langseth, Cecilie Bucher-Johannessen, Bastian Fromm, Andreas Keller, Eckart Meese, Marianne Lauritzen, Magnus Leithaug, Robert Lyle, and Trine B. Rounge. 2018. "A Comprehensive Profile of Circulating RNAs in Human Serum." *RNA Biology* 15 (2): 242–50.

Valiente-Pallejà, Alba, Helena Torrell, Gerard Muntané, Maria J. Cortés, Rafael Martínez-Leal, Nerea Abasolo, Yolanda Alonso, Elisabet Vilella, and Lourdes Martorell. 2018. "Genetic and Clinical Evidence of Mitochondrial Dysfunction in Autism Spectrum Disorder and Intellectual Disability." *Human Molecular Genetics* 27 (5): 891–900.

Wang, Huili, Sheng-Yan Lin, Fei-Fei Hu, An-Yuan Guo, and Hui Hu. 2020. "The Expression and Regulation of HOX Genes and Membrane Proteins among Different Cytogenetic Groups of Acute Myeloid Leukemia." *Molecular Genetics & Genomic Medicine* 8 (9): e1365.

Watahiki, Akira, Yuwei Wang, James Morris, Kristopher Dennis, Helena M. O'Dwyer, Martin Gleave, Peter W. Gout, and Yuzhuo Wang. 2011. "MicroRNAs Associated with Metastatic Prostate Cancer." *PloS One* 6 (9): e24950.

Yang, Chun, Seyed Nasrollah Tabatabaei, Xiangyan Ruan, and Pierre Hardy. 2017. "The Dual Regulatory Role of MiR-181a in Breast Cancer." *Cellular Physiology and Biochemistry: International Journal of Experimental Cellular Physiology, Biochemistry, and Pharmacology* 44 (3): 843–56.

Yu, Bin, Zhiyong Yang, Junjie Li, Svetlana Minakhina, Maocheng Yang, Richard W. Padgett, Ruth Steward, and Xuemei Chen. 2005. "Methylation as a Crucial Step in Plant microRNA Biogenesis." *Science* 307 (5711): 932–35.

Zhao, Lin-Yong, Jinghui Song, Yibin Liu, Chun-Xiao Song, and Chengqi Yi. 2020. "Mapping the Epigenetic Modifications of DNA and RNA." *Protein & Cell*, May. https://doi.org/10.1007/s13238-020-00733-7.

SUPPLEMENTARY FIGURES

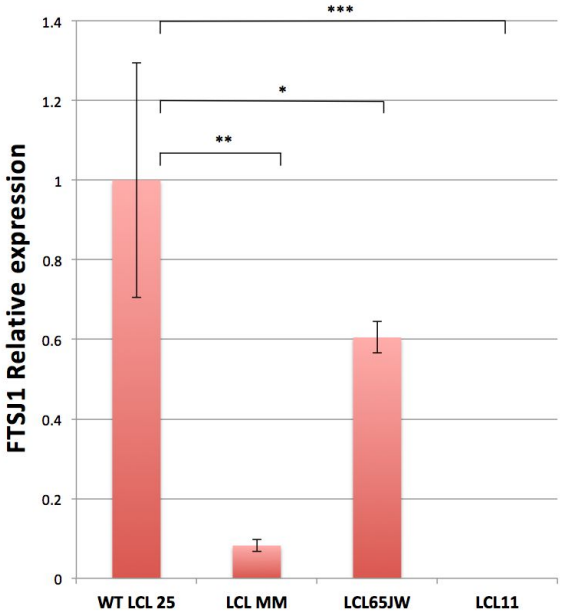

Figure S1a: FTSJ1 mRNA relative abundance in patient LCLs. FTSJ1 mRNA is significantly reduced in LCL MM compared to a control LCL. Relative abundance of mRNA is quantified by RT-qPCR on total RNAs from each indicated cell line. Ratios are expressed in fold change of starting quantities of FTSJ1/GAPDH. Error bars represent the standard deviation between four independent biological samples. P values are indicated with stars *p=0,04, **p=0,006, ***p=0,0008 (Paired Student's *t* test).

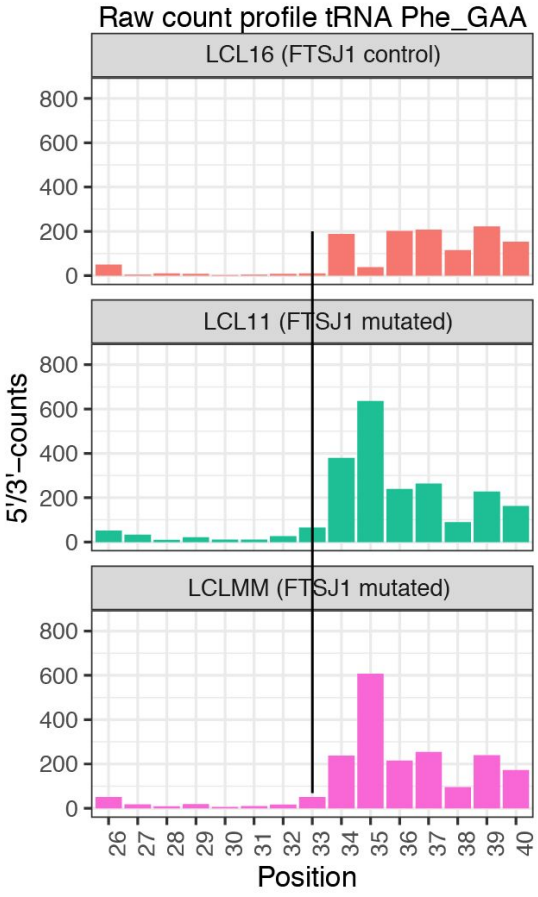

Figure S1b: FTSJ1 targets human tRNA$^{Phe(GAA)}$ at positions 32. Related to Figure. 1b. RiboMethSeq analysis of tRNA$^{Phe(GAA)}$ modification at positions Cm_{32} and Gm_{34} Alkaline fragmentation-based RiboMethSeq was performed on total RNAs extracted from indicated LCLs hemizygous mutants for *FTSJ1* (LCL11 and LCLMM) and control *FTSJ1* (non-mutated: LCL16*)* as indicated. For better visualization, raw read counts are presented in a non-normalized fashion (5'/3'-counts, raw count profil). The positions of interest (Cm_{32}) in tRNA$^{Phe(GAA)}$ is indicated by a black line crossing the 3 graphs.

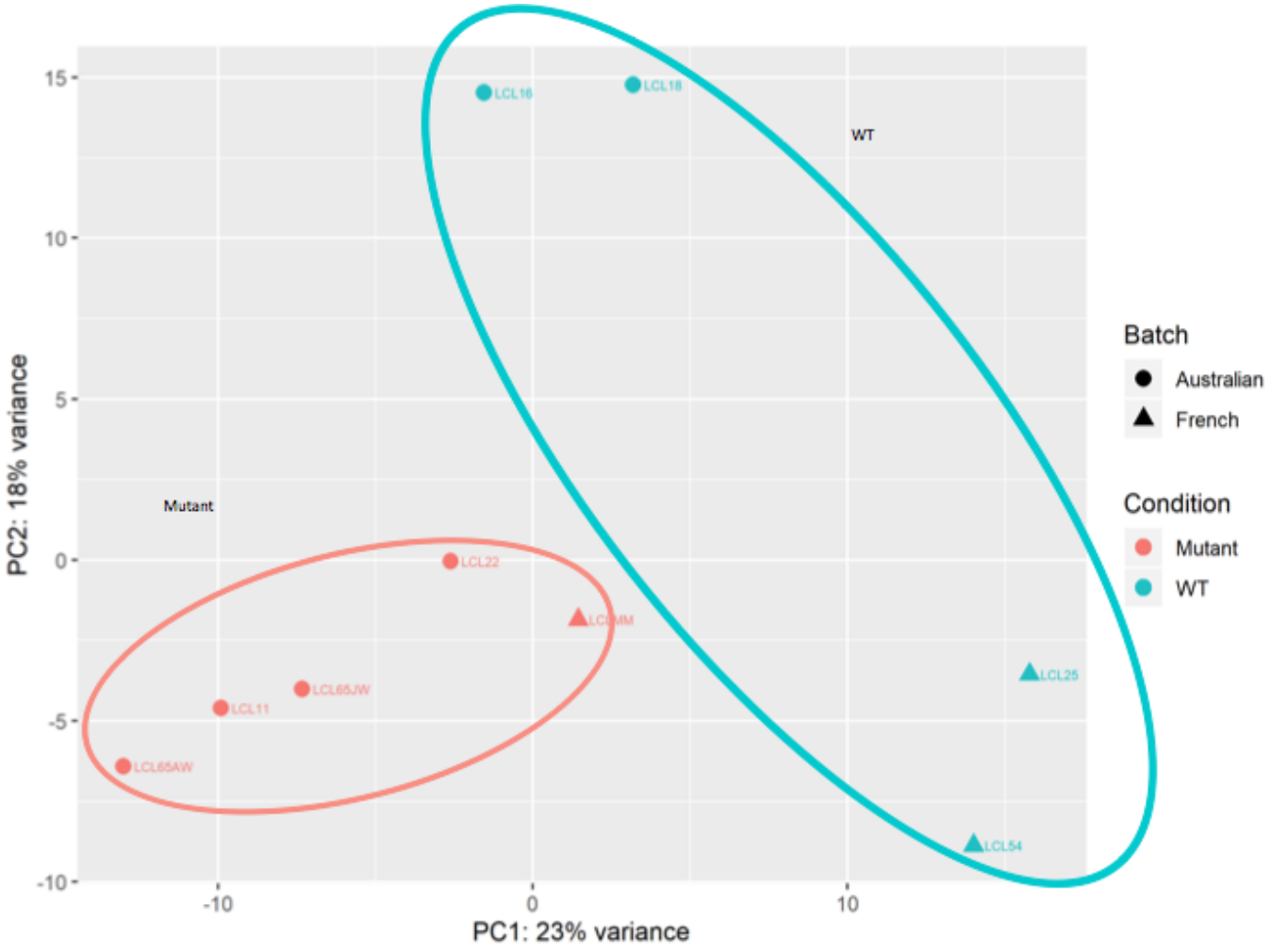

Figure S2a. FTSJ1 loss of function leads to miRNAs deregulation in NSXLID patients cells. The principal component analysis (PCA) plot shows a well-defined cluster of all LCL lines lacking FTSJ1 function that is separated from the more dispersed cluster of control lines (LCL WT for FTSJ1: WT; LCL Mutant for FTSJ1: Mutant).

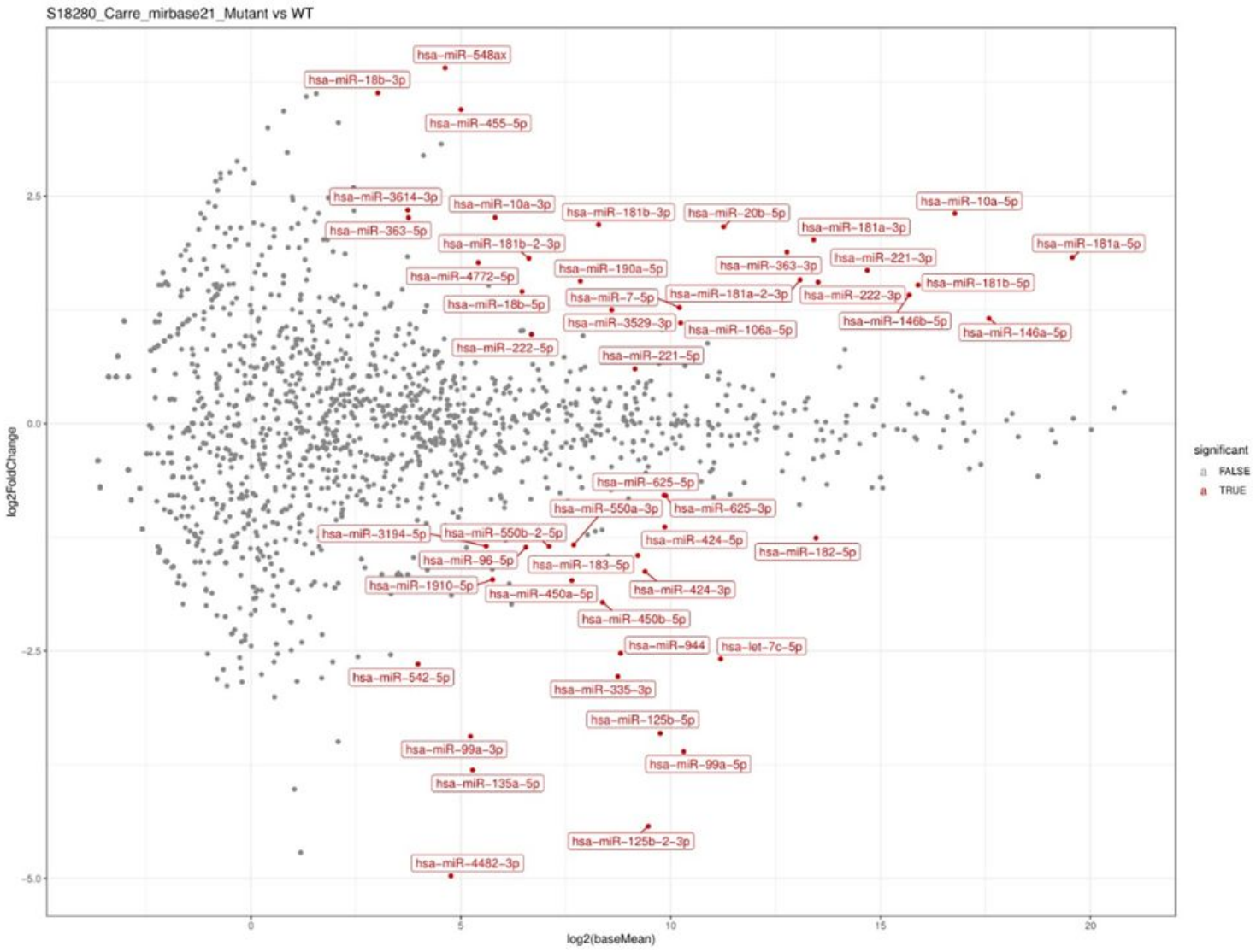

Figure S2b. FTSJ1 loss of function leads to miRNAs deregulation in NSXLID patients LCLs. MAplot on data from sequencing of miRNAs showing multiple deregulated miRNAs (LCL WT for FTSJ1: WT; LCL Mutant for FTSJ1: Mutant).

#	miRNA	baseMean_mutant	baseMean_wt	log2FoldChange Mutant_vs_WT	padj
1	hsa-miR-20b-5p	3987	538	2,16	1,21E-06
2	hsa-miR-222-3p	16116	6101	1,55	6,24E-06
3	hsa-miR-548ax	42	3	3,91	6,24E-06
4	hsa-miR-125b-2-3p	235	1295	-4,43	1,37E-05
5	hsa-miR-221-3p	37248	12664	1,68	3,76E-05
6	hsa-miR-335-3p	217	690	-2,78	7,92E-05
7	hsa-miR-181b-2-3p	142	44	1,82	7,92E-05
8	hsa-miR-99a-5p	538	2186	-3,61	0,0001
9	hsa-miR-10a-5p	161396	49508	2,31	0,0002
10	hsa-miR-181b-3p	472	111	2,18	0,0005
11	hsa-miR-106a-5p	1737	547	1,10	0,0005
12	hsa-miR-181a-2-3p	12183	4280	1,58	0,0009
13	hsa-miR-146a-5p	256346	121011	1,15	0,0009
14	hsa-miR-4482-3p	2	58	-4,97	0,0009
15	hsa-miR-125b-5p	468	1354	-3,41	0,0009
16	hsa-miR-450b-5p	235	454	-1,97	0,0009
17	hsa-miR-424-3p	608	750	-1,63	0,0012
18	hsa-miR-363-3p	10299	2814	1,88	0,0017
19	hsa-let-7c-5p	1044	3949	-2,59	0,0017
20	hsa-miR-450a-5p	157	254	-1,73	0,0020
21	hsa-miR-18b-5p	131	34	1,45	0,0033
22	hsa-miR-550a-3p	141	288	-1,33	0,0033
23	hsa-miR-181a-5p	1097695	379340	1,82	0,0033
24	hsa-miR-550b-2-5p	94	192	-1,35	0,0044
25	hsa-miR-181a-3p	15949	4441	2,02	0,0051
26	hsa-miR-181b-5p	83655	32365	1,52	0,0100
27	hsa-miR-183-5p	391	848	-1,45	0,0112
28	hsa-miR-99a-3p	24	55	-3,44	0,0134
29	hsa-miR-135a-5p	6	80	-3,81	0,0135
30	hsa-miR-146b-5p	70718	29704	1,41	0,0190
31	hsa-miR-542-5p	13	19	-2,65	0,0321
32	hsa-miR-944	138	833	-2,53	0,0376
33	hsa-miR-625-5p	707	1186	-0,79	0,0395
34	hsa-miR-625-3p	723	1220	-0,79	0,0412
35	hsa-miR-4772-5p	56	26	1,77	0,0420
36	hsa-miR-182-5p	8091	15213	-1,26	0,0473

Figure S2c. FTSJ1 loss of function leads to miRNAs deregulation in NSXLID patients LCLs. A list of the significantly deregulated miRNAs and their log2 fold change and adjusted p.value between FTSJ1 loss-of-function LCLs and control LCLs.

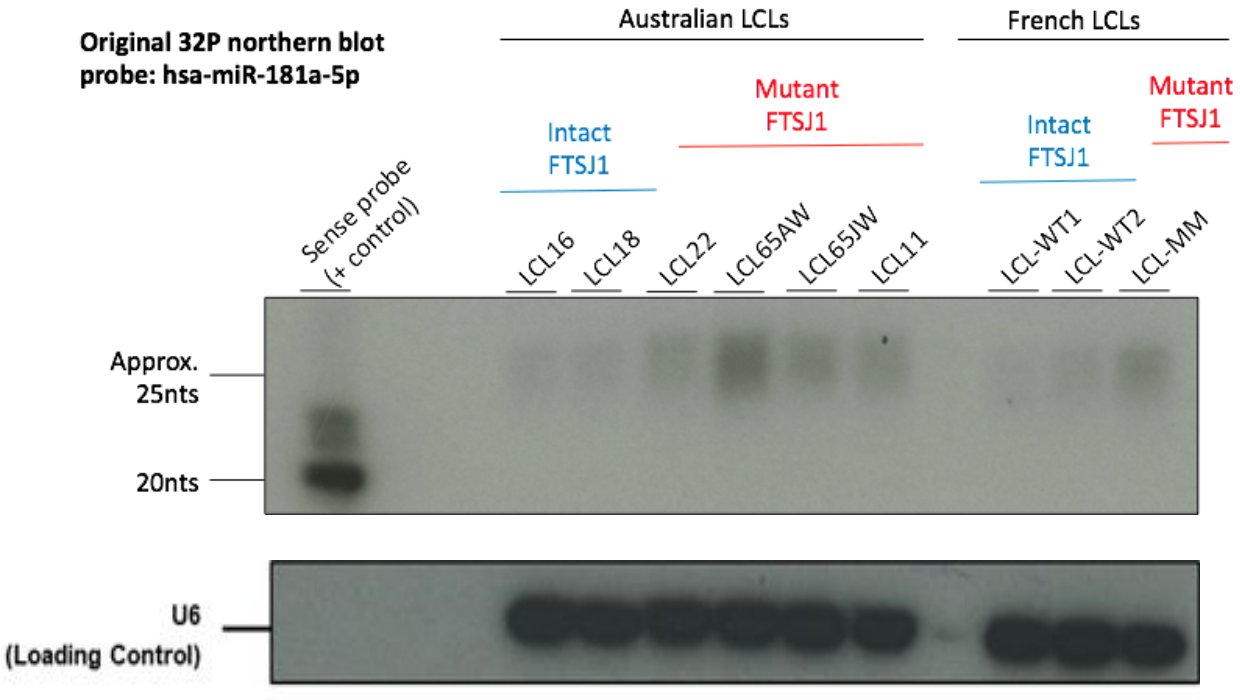

Figure S2d. FTSJ1 loss of function leads to miRNAs deregulation in NSXLID patients LCLs. Northern blot analysis with ^{32}P-labelled probe specific for hsa-miR-181a-5p confirms the upregulation of this miRNA in FTSJ1 loss of function condition already detected by small RNAseq analysis. Original scan of the blot exposure corresponding to the Figure. 2e.

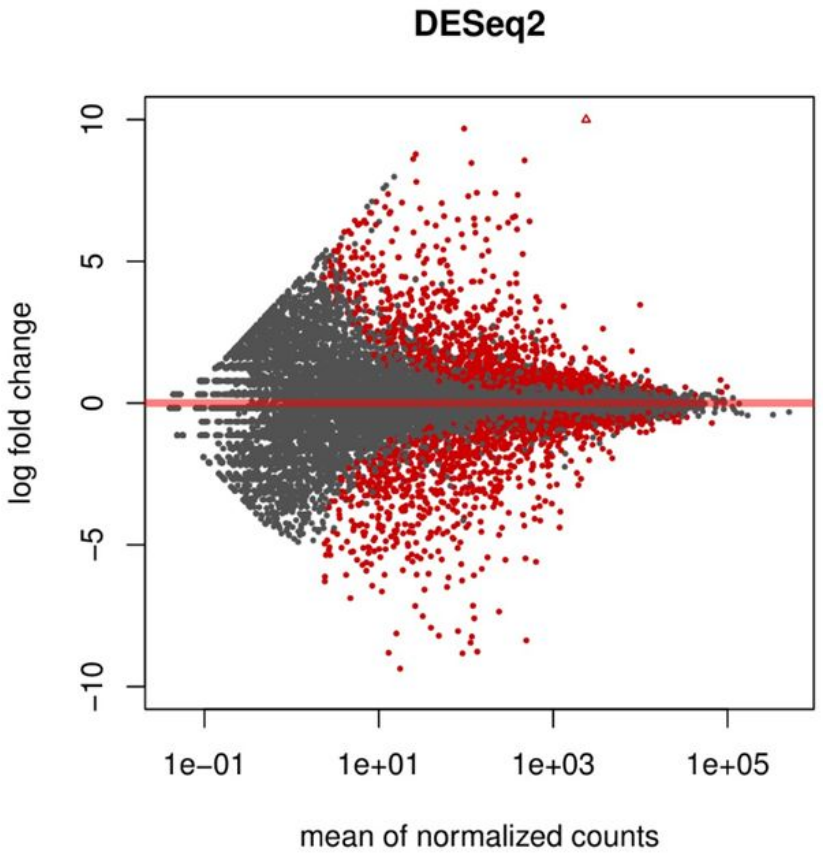

Figure S3a. FTSJ1 loss of function leads to mRNAs deregulation in NSXLID patients LCLs. MAplot on data from sequencing of mRNAs showing multiple deregulated mRNAs.

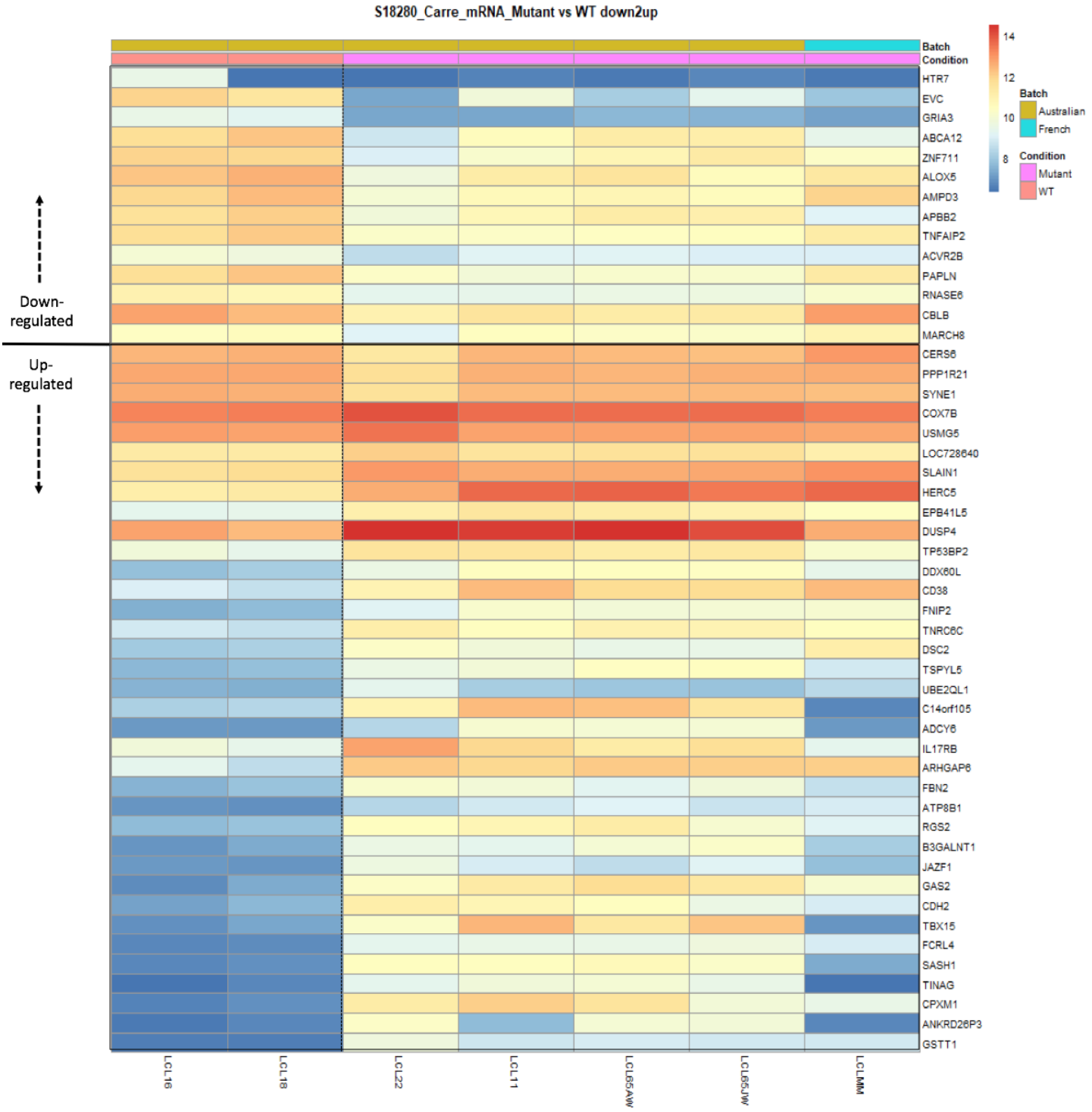

Figure S3b. FTSJ1 loss of function leads to mRNAs deregulation in NSXLID patients LCLs. Heat map showing the top 50 deregulated mRNAs in FTSJ1 loss of function LCLs compared to wild type FTSJ1 LCL. Batch points to the country of origin of the LCLs. Condition points to the FTSJ1 LCL status, WT or mutated for FTSJ1 gene.